A

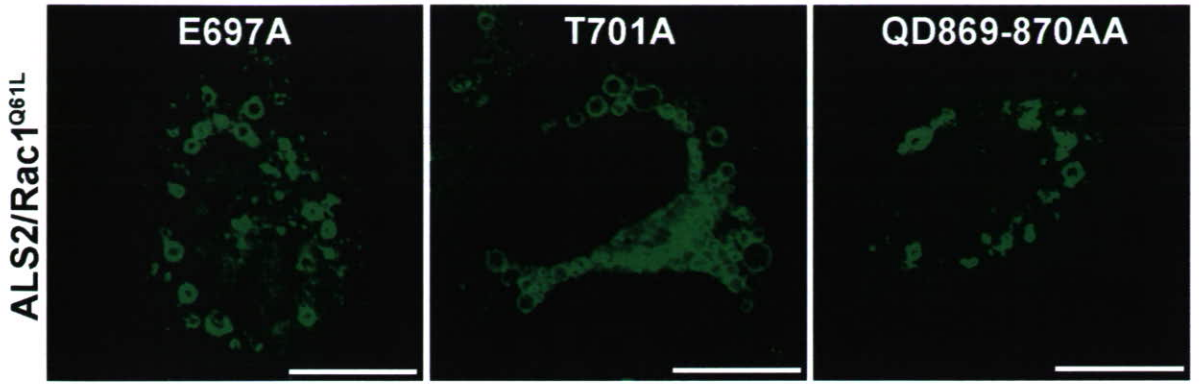

B

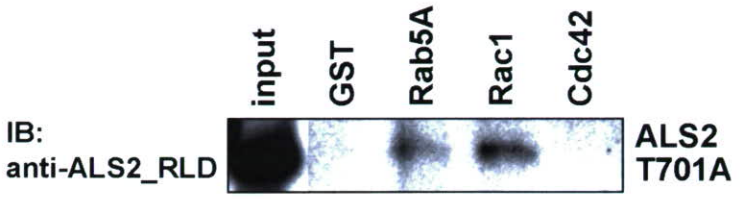

Supplementary Fig. 4 Kunita et al.

Available online at www.sciencedirect.com
ScienceDirect
Neurochemistry International 51 (2007) 74–84
NEUROCHEMISTRY International
www.elsevier.com/locate/neuint

Review

Molecular and cellular function of ALS2/alsin: Implication of membrane dynamics in neuronal development and degeneration

Shinji Hadano [a,b], Ryota Kunita [a], Asako Otomo [b], Kyoko Suzuki-Utsunomiya [b], Joh-E Ikeda [a,b,c,*]

[a] *Department of Molecular Life Sciences, Tokai University School of Medicine, Isehara, Kanagawa 259-1193, Japan*
[b] *Department of Molecular Neuroscience, The Institute of Medical Sciences, Tokai University, Isehara, Kanagawa 259-1193, Japan*
[c] *Department of Paediatrics, Faculty of Medicine, University of Ottawa, Ontario K1H 8M5, Canada*

Received 28 March 2007; received in revised form 18 April 2007; accepted 19 April 2007
Available online 4 May 2007

Abstract

ALS2 is a causative gene for a juvenile autosomal recessive form of motor neuron diseases (MNDs), including amyotrophic lateral sclerosis 2 (ALS2), juvenile primary lateral sclerosis, and infantile-onset ascending hereditary spastic paralysis. These disorders are characterized by ascending degeneration of the upper motor neurons with or without lower motor neuron involvement. Thus far, a total of 12 independent *ALS2* mutations, which include a small deletion, non-sense mutation, or missense mutation spreading widely across the entire coding sequence, are reported. They are predicted to result in either premature termination of translation or substitution of an evolutionarily conserved amino acid. Thus, a loss of functions in the *ALS2*-coded protein accounts for motor dysfunction and/or degeneration in the *ALS2*-linked MNDs. The *ALS2* gene encodes a novel 184 kDa protein of 1657 amino acids, ALS2 or alsin, comprising three predicted guanine nucleotide exchange factor (GEF) domains: the N-terminal RCC1-like domain, the central Dbl homology and pleckstrin homology (DH/PH) domains, and the C-terminal vacuolar protein sorting 9 (VPS9) domain. In addition, eight consecutive membrane occupation and recognition nexus (MORN) motifs are noted in the region between DH/PH and VPS9 domains. ALS2 activates Rab5 small GTPase and involves in endosome/membrane trafficking and fusions in the cells, and also promotes neurite outgrowth in neuronal cultures. Further, a neuroprotective role for ALS2 against cytotoxicity; i.e., the mutant Cu/Zn-superoxide dismutase 1 (SOD1)-mediated toxicity, oxidative stress, and excitotoxicity, has recently been implied. This review outlines current understandings of the molecular and cellular functions of ALS2 and its related proteins on safeguarding the integrity of motor neurons, and sheds light on the molecular pathogenesis of MNDs as well as other conditions of neurodegenerative diseases.

Keywords: Motor neuron disease; Amyotrophic lateral sclerosis; ALS2/alsin; Guanine nucleotide exchange factor (GEF); Small GTPase; Endosome dynamics

Contents

* Corresponding author at: Department of Molecular Life Sciences, Tokai University School of Medicine, 143 Shimokasuya, Isehara-city, Kanagawa 259-1193, Japan. Tel.: +81 463 91 5095; fax: +81 463 91 4993.
E-mail address: jeikeda3@is.icc.u-tokai.ac.jp (J.-E. Ikeda).

0197-0186/$ – see front matter © 2007 Elsevier Ltd. All rights reserved.
doi:10.1016/j.neuint.2007.04.010

1. Introduction

Motor neuron diseases (MNDs) is a group of disorders characterized by the selective dysfunction and/or loss of either upper motor neurons (UMNs), or lower motor neurons (LMNs), or both, leading to relentlessly progressive weakness with variable degrees, muscle atrophy with eventual paralysis, and in many cases to death. One of the best characterized and known form of MNDs is amyotrophic lateral sclerosis (ALS), in which both UMN and LMN are affected (Boillée et al., 2006; Pasinelli and Brown, 2006), and thus the term of MND and ALS are sometimes interchangeable. However, it is generally accepted that MNDs also include other forms of disorders resulting from the dysfunction confined to UMN, such as primary lateral sclerosis (PLS) and spastic paraplegia (spastic gait; SPG), and those involved in the selective degeneration of LMNs, such as spinal muscular atrophy (SMA) (Fink, 2001; Verma and Bradley, 2001; Shaw, 2005; Chevalier-Larsen and Holzbaur, 2006; Gros-Louis et al., 2006; James and Talbot, 2006; Simpson and Al-Chalabi, 2006).

Most cases of MND/ALS are sporadic, and thus their causes are largely unknown. To delineate the molecular pathogenesis for such diseases, the identification of genes and their mutations that link to the familial forms of MND/ALS is essential. Indeed, recent advances in human genetics and genomics greatly facilitate the chromosomal mapping of disease loci, and the identification of the causative genes and mutations predisposing to many familial forms of MNDs (Gros-Louis et al., 2006; James and Talbot, 2006). The following molecular characterizations of the disease-causing and -related gene products, in conjunction with the generation of animal disease models, have large impacts on a wide range of disease studies to date. More than 30 causative genes underlying MND/ALS have been identified thus far (reviews in Boillée et al., 2006; Chevalier-Larsen and Holzbaur, 2006; Gros-Louis et al., 2006; James and Talbot, 2006; Pasinelli and Brown, 2006; Simpson and Al-Chalabi, 2006). One of the hallmarks for the MND/ALS studies was the identification of mutations in the Cu/Zn superoxide dismutase 1 (SOD1) gene as a cause for the autosomal dominant ALS with adult onset (ALS1) (Rosen et al., 1993). In this review, we focus on the second ALS-related gene, *ALS2*. The *ALS2* gene was originally identified by positional cloning, and the mutations in the *ALS2* gene account for a juvenile forms of autosomal recessive MND/ALS (Hadano et al., 2001a; Yang et al., 2001).

2. The *ALS2* gene

2.1. Mutation

ALS2 (OMIM 205100), also known as type 3 autosomal recessive ALS (RFALS type3), was originally reported in a large consanguineous Tunisian kindred and was characterized by a loss of UMNs and spasticity of limb and facial muscles accompanying distal amyotrophy of hands and feet (Ben-Hamida et al., 1990). The *ALS2* locus has been mapped to the 1.7 cM interval flanked by *D2S116* and *D2S2237* on chromosome 2q33 by linkage and haplotype analyses (Hentati et al., 1994; Hosler et al., 1998). The following physical cloning and mapping revealed that this interval spanned approximately 3 Mb of genomic DNA (Hosler et al., 1998; Hadano et al., 1999, 2001b), and allowed the generation of a transcript map of the *ALS2* critical region (Hadano et al., 2001a,b). In 2001, the *ALS2* (initially designated as *ALS2CR6*) gene was identified as a causative gene for ALS2 (Hadano et al., 2001a; Yang et al., 2001). At the same time, two additional *ALS2* mutations were found in patients with a rare juvenile recessive form of PLS (PLSJ; OMIM 606353) in both Kuwaiti and Saudi Arabian consanguineous families (Hadano et al., 2001a; Yang et al., 2001). Recently, although mutations or variations in the *ALS2* gene are not a common cause of sporadic or familial ALS (Al-Chalabi et al., 2003; Hand et al., 2003; Nagano et al., 2003), several independent homozygous *ALS2* mutations have been found in families segregating an infantile-onset ascending hereditary spastic paralysis (IAHSP; OMIM 607225) (Devon et al., 2003; Eymard-Pierre et al., 2002, 2006; Lesca et al., 2003; Panzeri et al., 2006), a single family of a recessive complicated hereditary spastic paraplegia (HSP) (Gros-Louis et al., 2003), and a single family of ALS2 (Kress et al., 2005). Thus far, a total of 12 independent *ALS2* mutations, which include the small deletions, non-sense mutations, or missense mutations spreading widely across the entire coding sequence, are reported (Table 1). These mutations are predicted to result in either premature termination of translation or substitution of an evolutionarily conserved amino acid. Since ALS2, PLSJ, and IAHSP/HSP are group of closely related recessive MNDs, and a loss of functions in the *ALS2* mutations may account for a number of recessive MNDs, it is likely that the *ALS2*-coded protein bears on maintaining the integrity of motor neurons.

2.2. Structure and expression

The *ALS2* gene comprises 33 introns and 34 exons and resides within 80.3 kb of genomic DNA on chromosome 2q33. Sequence of the *ALS2* transcript encompasses 6394 nucleotides (nt) with a single open reading frame (ORF: 4974 nucleotides long, 124–5097 nt), and is predicted to encode a 184 kDa protein consisting of 1657 amino acids (aa). A shorter transcript for *ALS2* (*ALS2_S*) that encompasses 2651 nt with a single 1191 nt ORF encoding 396 aa. The *ALS2_S* transcript is a product of alternative splicing at the 5′ donor site after exon 4, resulting in a premature stop codon after 25 amino acid residues in intron 4. Consistent with these findings, two transcripts of approximately

Table 1
Mutations in the *ALS2* gene in *ALS2*-linked motor neuron diseases

Mutations (Transcript or gene)[a]	Location	Type[b]	Mutant proteins[a]	Origin	Disease[c]	Phenotype[d]	References
c.138delA	Exon 3	fs	A47fsX4	Tunisian	ALS2	U/L	Hadano et al. (2001a) and Yang et al. (2001)
c.470G>A	Exon 4	ms	C157Y	Turkish	IAHSP	U	Eymard-Pierre et al. (2006)
c.553delA	Exon 4	fs	T185fsX5	Turkish	ALS2	U/L	Kress et al. (2005)
c.1007_1008delTA	Exon 4	fs	I336fsX5	Italian	IAHSP	U	Eymard-Pierre et al. (2002)
c.1425_1426delAG	Exon 5	fs	G476fsX71	Kuwaiti	PLSJ	U	Hadano et al. (2001a)
IVS5(c.1472)-1G>T(C.1472_1481delTTTCCCCCAG)	Intron 5	fs	V491fsX3	French	IAHSP	U	Eymard-Pierre et al. (2002)
c.1619G>A	Exon 6	ms	G540E	Italian	PLSJ	U	Panzeri et al. (2006)
c.1867_1868delCT	Exon 9	fs	L623fsX24	Saudi Arabian	PLSJ	U	Yang et al. (2001)
c.2537_2538delAT	Exon 13	fs	N846fsX13	Italian	IAHSP	U	Eymard-Pierre et al. (2002)
c.2992C>T	Exon 18	ns	R998X	Israeli	IAHSP	U	Devon et al. (2003)
c.3619delA	Exon 23	fs	M1207X	Algerian	IAHSP	U	Eymard-Pierre et al. (2002)
c.4721delT	Exon 32	fs	V1574fsX44	Pakistani	IAHSP	U	Gros-Louis et al. (2003)

[a] The description of the mutations are accorded by den Dunnen and Antonarakis (Hum Mut 15, 7–12, 2000).
[b] fs: frame shift, ms: missense, ns: nonsense.
[c] ALS2: amyotrophic lateral sclerosis 2 (OMIM 205100), PLSJ: juvenile primary lateral scelrosis (OMIM 606353), IAHSP: infantile-onset ascending hereditary spastic paralysis (OMIM 607225).
[d] U: upper motor neuron involvement, L: lower motor neuron involvement.

6.5 and 2.6 kb in various adult human tissues are detected by Northern blot analysis (Hadano et al., 2001a). Both transcripts are expressed ubiquitously with highest in the central nervous system (CNS), particularly in the cerebellum.

Murine ortholog for *ALS2*, officially designated as *Als2*, encompasses 6349 nt with a single ORF that is 4956 nt long (124–5079 nt), and is predicted to encode a 183 kDa protein consisting of 1651 aa. The entire ORF is well conserved between human and mouse (87% identity at DNA level). The *Als2* short variant (*Als2_S*) of a 2955 nt with a single 2787-nt ORF encoding 928 aa (~100 kDa), which is produced by alternative splicing at the 5′ donor site after exon 13, resulting in a premature stop codon after 74 amino acid residues in intron 13. Thus, the structure of the mouse *Als2_S* transcript is different from that of the human variant (Hadano et al., 2006). In adult mouse CNS, the *Als2* transcript is expressed to a variable degree in neuronal cells throughout the brain and spinal cord, particularly in neurons in the hippocampus, cerebellum, cerebral cortex, spinal gray matter (motor neurons), olfactory bulb, basal ganglia, and cranial nuclei (Hadano et al., 2001a) with most abundant in the granular layer of the cerebellum (Devon et al., 2005; Lein et al., 2007; Allen Brain Atlas, http://www.brain-map.org/welcome.do). During development, *Als2* expression is limited at an early embryonic stage (E9.5–E12.5), but is gradually increased in CNS after E14.5 and reaches adult levels at P7 (Devon et al., 2005), reflecting that *Als2* implicates in neuronal development.

3. The ALS2 protein (ALS2/alsin)

The human *ALS2* and mouse *Als2* genes encodes proteins of 1657 aa and 1651 aa, respectively, which are called ALS2 (Hadano et al., 2001a) or alsin (Yang et al., 2001). Analysis of the predicted amino acid sequences identified a high level of sequence similarity throughout the entire region of human and mouse ALS2 proteins (91% identity, 94% similarity). Database searches demonstrate the presence of orthologs in vertebrates as well as in fry (*D. melanogaster*; CG7158) and mosquito (*A. gambiae*), but not in nematode (*C. elegans*) and yeast (Devon et al., 2005). A number of interesting domains and motifs in the deduced ALS2 protein sequence is noted (Fig. 1). A region in the N-terminal half of ALS2 is highly homologous to regulator of chromosome condensation (RCC1) and retinitis pigmentosa GTPase regulator (RPGR) including its functional structural motif; a seven-bladed propeller (Hadano et al., 2001a; Topp et al., 2004). This domain is referred as to RCC1-like domain (RLD). RCC1 is a guanine nucleotide exchange factor (GEF) for the nuclear GTP binding protein Ran (Ras-related nuclear) (Dasso, 2001). A middle portion of ALS2 contains a tandem organization of a diffuse B cell lymphoma (Dbl) homology (DH) and pleckstrin homology (PH) domains, that is a hallmark of GEFs for Rho (Ras homologous member)-type GTPases (Rossman et al., 2005). The vacuolar protein sorting 9 (VPS9) domain, which has been found in a number of Rab5 (Ras-related in brain 5) GEFs (Zerial and McBride, 2001; Carney et al., 2006), is also found in the C-terminal region. In addition, a tandem array of eight membrane occupation and recognition nexus (MORN) motifs each consisting of 23 amino acids (Takeshima et al., 2000), which is implicated in the binding of plasma membranes, are also noted in the region between the DH/PH and VPS9 domains.

ALS2 is predominantly expressed in CNS with highest in the cerebellum, consistent with an expression pattern of the *ALS2*/*Als2* mRNA. Expression of ALS2 in non-CNS organs and tissues was generally low, except for in the testis (Hadano et al., 2006; Devon et al., 2006). A series of differential centrifugation experiments using brain tissues have revealed that ALS2 is enriched in P3 membrane fractions where a number of endosomal proteins, such as transferrin (Tf) receptor, early endosome auto-antigen 1 (EEA1), and synaptophysin, are co-fractionated, suggesting that ALS2 is predominantly distributed

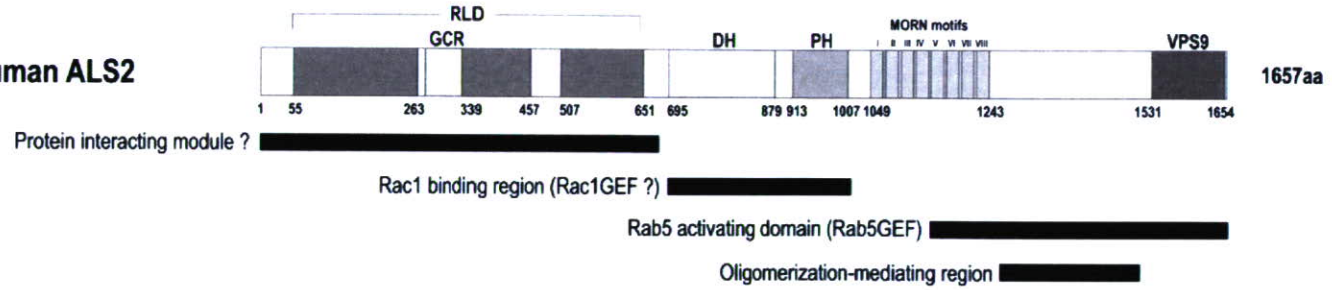

Fig. 1. Schematic representation of the human full-length ALS2 protein (ALS2) and its domains and motifs. ALS2 contains three predicted guanine nucleotide exchange factor (GEF) domains; i.e., RCC1-like domain (RLD), diffuse B cell lymphoma (Dbl) homology (DH) and pleckstrin homology (PH) domains, and vacuolar protein sorting 9 (VPS9) domain. In addition, eight consecutive membrane occupation and recognition nexus (MORN) motifs are noted in the region between DH/PH and VPS9 domains. GCR stands for glucocorticoid receptor homologous region. A number of the functionally assigned regions are also noted.

to endosomal membrane compartments (Yamanaka et al., 2003; Topp et al., 2004; Devon et al., 2005). Notably, a significant amount of ALS2 is also present both in P2 (mitochondrial/synaptosomal) and S3 (soluble) fractions (Suzuki-Utsunomiya et al., unpublished). Further, it has been shown that ALS2 is enriched in a centrosome preparations purified from human cortical brain (Millecamps et al., 2005).

Immunohistochemical analysis of ALS2 using anti-ALS2 antibodies combined with neuronal and glial markers have revealed that ALS2 is expressed in various neurons, but not glial cells in mice (Hadano et al., 2006), consistent with the mRNA *in situ* hybridization studies. ALS2 is highly expressed in the granular layers of the cerebellum (Devon et al., 2005; Hadano et al., 2006), and shows the colocalization with some, but not all calbindin immunopositive Purkinje cells (Hadano et al., 2006). High magnification studies have demonstrated that ALS2 is mainly distributed in a diffused manner, but several dot or patchy stainings are consistently observed in soma as well as in dendrite, suggesting that ALS2 localizes not only in the cytosol but also onto vesicular and/or membranous compartments in neurons (Hadano et al., 2006). However, as there are still inconsistencies in the results of the immunohistochemical ALS2 localization (Devon et al., 2005; Hadano et al., 2006), further careful assessments will be required.

It is noted that there is currently no evidences for the expression of the expected truncated protein products in lymphoblasts from patients with confirmed homozygous mutation in *ALS2* (Yamanaka et al., 2003) and short variants of the *ALS2/Als2* genes (Otomo et al., 2003; Yamanaka et al., 2003; Hadano et al., 2006). Interestingly, both the mutated ALS2 and a naturally truncated isoform of ALS2 (*ALS2_S*) proteins are rapidly degraded in human cultured cells (Yamanaka et al., 2003; Eymard-Pierre et al., 2006), suggesting that loss of function coupled with protein instability may, in part, account for the pathogenesis underlying the ALS2-linked MNDs.

4. Function of ALS2

4.1. Biochemical characteristics

The small GTPases act as binary switches by cycling between an inactive (GDP-bound) and an active (GTP-bound) state, and regulate a broad spectrum of cellular and molecular processes. GEFs are known to stimulate the exchange of GDP for GTP, thereby generating the active forms of the small GTPases (Vetter and Wittinghofer, 2001). For example, RCC1 (RanGEF) activates Ran GTPase, which implicates in nuclear transfer as well as chromatin condensation through the regulation of microtubule assembly (Dasso, 2001). The Rho subfamilies, which are activated by the DH/PH (Rossman et al., 2005) or DOCK (Côté and Vuori, 2002) -containing GEFs, are critical regulators of the organization of the actin cytoskeleton, various signaling cascades, and neuronal morphogenesis (Da Silva and Dotti, 2002; Etienne-Manneville and Hall, 2002; Luo, 2000; Snider et al., 2002; Van Aelst and Symons, 2002). Further, the Rab GTPases have emerged as key players for the vesicle budding, motility/trafficking, fusion, and signal transduction (Zerial and McBride, 2001; Miaczynska et al., 2004). In particular, the VPS9 domain-containing GEFs are shown to activate the Rab5 family of GTPases (Carney et al., 2006).

Since ALS2 contains multiple putative GEF domains; RLD, DH/PH, and VPS9, implying that ALS2 acts as a regulator/activator of multiple small GTPases (Hadano et al., 2001a; Yang et al., 2001). However, *in vitro* GDP dissociation and GTP binding assays (i.e., GEF assays) proved that ALS2 exhibits selective GEF activity on the members of Rab5 family (Rab5A, Rab5B, and Rab5C), but neither on other members of GTPases including Rab family (Rab3, Rab4, Rab7, Rab9, and Rab11), Arf family (ARF1 and ARF6), Rho family (Rac1, Cdc42, and RhoA), nor Ran (Otomo et al., 2003; Topp et al., 2004). Thus, ALS2 acts as a specific GEF for the Rab5 GTPase family *in vitro*. A series of the *in vitro* Rab5-GEF assays using the N- and C-terminally truncated ALS2 fragments reveals a region conferring the ALS2-associated Rab5GEF activity to the C-terminal half of ALS2 that contains the MORN-VPS9 domains. Lack of either the MORN motifs or VPS9 domain results in the loss of the Rab5-GEF activity (Otomo et al., 2003). Mutations in an evolutionarily conserved amino acid residue within the VPS9 domain; i.e., ALS2_P1603A and ALS2_L1617A, result in a marked decrease in the ALS2-associated Rab5-GEF activity (Otomo et al., 2003). Intriguingly, ALS2 forms a homophilic oligomer through two distinct C-terminal regions mapped within the interval between MORN motifs and VPS9 domain, which is crucial for the ALS2-associated Rab5 GEF

activity (Kunita et al., 2004). Moreover, the C-terminal region of ALS2 mediates the direct interaction between ALS2 and Rab5A (Otomo et al., 2003; Kunita et al., 2004; Hadano and Ikeda, 2005). Taken together, every element in the C-terminal ALS2 might be the determinant for the structural context of ALS2 that are indispensable for the ALS2-asociated Rab5 GEF activity (Fig. 1).

Notably, there are additional genes encoding members of the Rab5 family, including Rab21, Rab22a, Rab31 (Rab22b), and Rab22c, other than Rab5A, Rab5B, and Rab5C, in the human genome (Stenmark and Olkkonen, 2001). Recently, Rabex-5, the well-studied VPS9 domain-containing Rab5GEF, has been shown to activate not only Rab5 but also Rab21 and Rab22a (Delprato et al., 2004). Further, another VPS9 domain-containing proteins, Varp and Gapex-5, exhibits a predominant catalytic activity on Rab21 and Rab31, respectively (Zhang et al., 2006; Lodhi et al., 2007). These findings suggest that each member of the VPS9-domain containing Rab5GEFs has a distinct catalytic property on the Rab5 GTPase family. The VPS9 domain-containing ALS2 protein also behaves as a GEF for Rab22a and Rab31 but not for Rab21 (Hadano et al., unpublished).

ALS2 contains the DH/PH domain in the middle, which is a hallmark of GEFs for Rho GTPase family. Indeed, it has been shown that ALS2 specifically binds to Rac1 *in vitro* in a DH/PH-domain dependent manner, but neither to Rac2, Rac3, Cdc42, RhoA, RhoB, RhoC, nor RhoG (Topp et al., 2004; Kanekura et al., 2005; Kunita et al., 2007). Further, overexpression of ALS2 in cultured cells marginally enhances the level of active Rac1, implying a potency of ALS2 to activate Rac1 (Topp et al., 2004; Kanekura et al., 2005; Tudor et al., 2005). However, as earlier mentioned, ALS2 does not possess the GEF activity on Rac1 *in vitro* (Otomo et al., 2003; Topp et al., 2004). Thus, the ALS2-associated Rac1GEF activity is still matter of conjecture (Fig. 1). Most recently, we have shown that ALS2 turns to be activated by Rac1, and thus ALS2 is a Rac1 effector rather than Rac1GEF (Kunita et al., 2007).

The N-terminal RLD of ALS2 conserves a seven-bladed propeller sequence that is a distinguishing feature of RCC1 as a Ran GEF (Hadano et al., 2001a; Topp et al., 2004). However, no significant ALS2-associated Ran GEF activity was detected *in vitro* (Otomo et al., 2003). Since RLDs are identified in many other proteins of diverse functions, the RLD in ALS2 might function as an interface between protein–protein or protein–lipid bindings rather than GEF (Fig. 1). Indeed, the ALS2-RLD modulates the association of ALS2 molecules to the membrane compartments (Yamanaka et al., 2003; Kunita et al., 2007). Further, the N-terminal region containing the RLD directly interacts with the C-terminal portion of ALS2, modulating the ALS2 distribution and activity in the cells (Kunita et al., 2007).

4.2. Cellular biological characteristics

In non-neuronal cultured cells, such as HeLa and COS-7 cells, ectopically expressed ALS2 diffusedly distributes throughout cytoplasm with occasional localization to small vesicular structures in the perinuclear region and to the leading membrane edges of cellular peripheries (Otomo et al., 2003). Similar distribution profiles of endogenous ALS2 in NIH3T3 cells are observed (Topp et al., 2004). Vesicular ALS2 is partially colocalized with Rab5 and EEA1, markers for endosomes, indicating that ALS2 is the endosomal tribe (Otomo et al., 2003; Topp et al., 2004). Indeed, a loss of ALS2 results in the delayed fusion of epidermal growth factor (EGF)-positive endosomes in mouse embryonic fibroblasts (MEFs) (Hadano et al., 2006), supporting that endogenous ALS2 serves in Rab5-dependent endosome fusion (Fig. 2). Remarkably, ALS2 molecules on the leading membrane edges and ruffles significantly overlap with Rac1 (Topp et al., 2004). In a subset of cultured cells, some of ALS2 molecules are colocalized with the centrosomal markers, such as γ-tubulin and A kinase anchoring protein (AKAP-450) (Millecamps et al., 2005). It has also been reported that overexpression of ALS2 not only results in an abnormal endosomal phenotypes, but also in impairment of mitochondria trafficking and fragmentation of the Golgi apparatus (Millecamps et al., 2005). Thus, ALS2 is fairly committed in a wide range of membrane dynamics and cytoskeletal organizations in the cells.

A series of experiments using cultured cells expressing a truncated as well as missense ALS2 mutants has revealed that each ALS2 domain/region demonstrates specific subcellular tropism *in vivo* (Otomo et al., 2003; Yamanaka et al., 2003; Topp et al., 2004). The C-terminus of ALS2 carrying the MORN/VPS9 domains activates Rab5, and also mediates the endosomal localization for ALS2. On the other hand, the N-terminal RLD, in a context of full-length ALS2, acts suppressive in the membranous localization of ALS2 itself (Otomo et al., 2003), although the RLD-containing fragment itself associates with the membranous structures under certain conditions (Yamanaka et al., 2003; Kunita et al., 2007). Notably, the DH/PH domain constitutively promotes the MORN/VPS9 domain-mediated Rab5 activation and endosome fusions *in vivo* (Otomo et al., 2003). Further, the homo-oligomerization of ALS2 through its C-terminal regions is crucial for this ALS2-mediated endosome enlargement (Kunita et al., 2004). These findings suggest that the intracellular localization of ALS2 and its-associated Rab5GEF activity seem to be controlled by the internal domain(s) of ALS2, probably through the association with ALS2 itself and/or other protein or lipid molecules. Indeed, a pathogenic missense mutation in the RLD of ALS2 that results in the ALS2 mislocalization; i.e., loss of endosomal ALS2, has been reported (Panzeri et al., 2006). Thus, proper arrangement of the ALS2 subcellular localization may be crucial to exert the physiological ALS2 functions.

In neurons, endogenous and overexpressed ALS2 are found primarily on small vesicular/punctate structures both in cell bodies and in elaborated somato-dendritic neurites of embryonic cortical, hippocampal, and motor neuronal cultures (Otomo et al., 2003; Topp et al., 2004; Jacquier et al., 2006). Some cytoplasmic ALS2 stainings are also observed (Otomo et al., 2003; Topp et al., 2004). At a matured stage of cultured neurons, vesicular ALS2 is present in either dendrites, axons, or the cell bodies, with no apparent polarized localization (Topp et al., 2004). Co-localization studies with Rab5 and EEA1

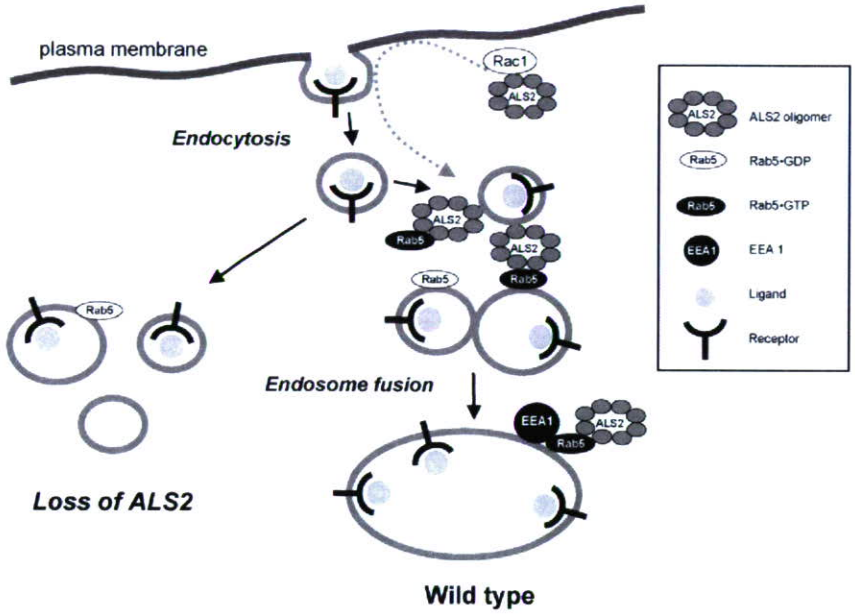

Fig. 2. Schematic representation of a model for the intracellular function of ALS2. ALS2 mediates Rab5-dependent endosome fusion in the cells. A particular molecular signal(s) (e.g., Rac1) activates and recruits the ALS2 oligomer to early endosomal compartments through Rac1-activated macropinocytosis (Kunita et al., 2007), wherein ALS2 binds to Rab5 GTPase. ALS2 activates Rab5 via its associated Rab5GEF activity. Activated Rab5 (Rab5-GTP) further facilitates the formation of protein complex comprising downstream effector molecules such as early endosome auto-antigen 1 (EEA1) and soluble *N*-ethylmaleimide-sensitive factor attachment protein receptor (SNARE) proteins (not shown), and promotes endosome fusion. A loss of ALS2 may perturb endosomal trafficking and fusion, thereby leading to dysfunction of intracellular molecular signaling; e.g., insulin-like growth factor 1 (IGF1) or brain-derived neurotrophic factor (BDNF) (see text), and ultimately resulting in dysfunction/degeneration of neuronal cells.

demonstrate that ALS2 is present in endosomal compartments in neurons (Otomo et al., 2003). On the other hands, at an immature stage, ALS2 is enriched on the tip of axon with a dense localization to Rac1/actin-positive lamellipodia and vesicles at growth cones (Tudor et al., 2005; Jacquier et al., 2006). Compelling evidences for the functional aspects of ALS2 in neuronal endosome dynamics have been obtained from two independent studies. The Rab5-dependent fusion activity is significantly reduced in the brain cytosol from the *Als2* knockout (KO) mice in comparison with wild-type (Devon et al., 2006). Further, siRNA-mediated knockdown of rat *Als2* in cultured motor neurons results in smaller-sized EEA1-positive endosomes (Jacquier et al., 2006). Thus, endogenous ALS2 certainly plays an important role in Rab5-dependent endosome fusion in neurons. On the other hand, studies using the ALS2 overexpression as well as *Als2* knockdown in conjunction with co-expression of the small GTPase have revealed that ALS2 stimulates neurite and axonal outgrowth in a Rac1-dependent manner (Tudor et al., 2005; Jacquier et al., 2006), suggesting that ALS2 enriched in growth cones may act as a modulator for neurite development. Collectively, ALS2 plays a role in membrane/vesicular trafficking and axonal outgrowth in neurons (Fig. 3), albeit the molecular linkages of these cellular events are still unclear.

4.3. ALS2 knockout mice

Als2 KO mice have been reported by five independent groups (Cai et al., 2005; Hadano et al., 2006; Devon et al., 2006; Yamanaka et al., 2006; Julien and Kriz, 2006). First two-lines of *Als2* KO mice were created by replacing the 39 bp of a *Bam*HI fragment in exon 3 with the *LacZ-NEO* cassette (Cai et al., 2005) and the stop codon followed by the *NEO* cassette (Hadano et al., 2006), respectively. Although the *Als2* gene in a targeted allele can be transcribed by its own promoter, the normal protein translation is terminated after first 14 amino acids, resulting the peptide lacks all the functional domains of ALS2. Third line was generated by using promoter trap gene targeting to replace exons 3 and 4 with SA-IRES-βgeo-pA cassette encoding bifunctional *LacZ*-neomycin fusion protein (Devon et al., 2006), and expected to produce fusion protein carrying only seven amino acid residues originated from ALS2 at the N-terminus. Forth line was produced by replacing exon 2 and part of exon 3 with the *NEO* cassette, resulting in a complete lack of transcription for the *Als2*-coded sequence (Julien and Kriz, 2006). Final line reported contain the *Als2*-null allele generated by replacing the 3′-half of exon 4 and intron 4 with the *NEO* cassette, which results in a truncated ALS2 peptide (174 aa) containing a portion of the N-terminal RLD (Yamanaka et al., 2006). Although there are slight differences in the gene targeting strategy, the translation of the full-length functional ALS2 protein is completely disrupted in all these mice (i.e., *Als2* KO mice) (Cai et al., 2005; Hadano et al., 2006; Devon et al., 2006; Yamanaka et al., 2006; Julien and Kriz, 2006).

Surprisingly, these studies combined demonstrate that absence of ALS2 does not develop *ALS2*-related disease phenotypes in mice; they show no obvious developmental and reproductive abnormalities with normal life-span. However, *Als2* KO mice exhibit age-dependent deficits in motor

References

Al-Chalabi, A., Hansen, V.K., Simpson, C.L., Xi, J., Hosler, B.A., Powell, J.F., McKenna-Yasek, D., Shaw, C.E., Leigh, P.N., Brown Jr., R.H., 2003. Variants in the *ALS2* gene are not associated with sporadic amyotrophic lateral sclerosis. Neurogenetics 4, 221–222.

Ben-Hamida, M., Hentati, F., Ben-Hamida, C., 1990. Hereditary motor system diseases (chronic juvenile amyotrophic lateral sclerosis). Brain 113, 347–363.

Boillée, S., Vande Velde, C., Cleveland, D.W., 2006. ALS: a disease of motor neurons and their nonneuronal neighbors. Neuron 52, 39–59.

Cai, H., Lin, X., Xie, C., Laird, F.M., Lai, C., Wen, H., Chiang, H.C., Shim, H., Farah, M.H., Hoke, A., Price, D.L., Wong, P.C., 2005. Loss of ALS2 function is insufficient to trigger motor neuron degeneration in knockout mice but predisposes neurons to oxidative stress. J. Neurosci. 25, 7567–7574.

Carney, D.S., Davies, B.A., Horazdovsky, B.F., 2006. Vps9 domain-containing proteins: activators of Rab5 GTPases from yeast to neurons. Trends Cell Biol. 16, 27–35.

Chevalier-Larsen, E., Holzbaur, E.L.F., 2006. Axonal transport and neurodegenerative disease. Biochim. Biophys. Acta 1762, 1094–1108.

Cooper, A.A., Gitler, A.D., Cashikar, A., Haynes, C.M., Hill, K.J., Bhullar, B., Liu, K., Xu, K., Strathearn, K.E., Liu, F., Cao, S., Caldwell, K.A., Caldwell, G.A., Marsischky, G., Kolodner, R.D., Labaer, J., Rochet, J.C., Bonini, N.M., Lindquist, S., 2006. α-Synuclein blocks ER-Golgi traffic and Rab1 rescues neuron loss in Parkinson's models. Science 313, 324–328.

Côté, J.-F., Vuori, K., 2002. Identification of an evolutionarily conserved superfamily of DOCK180-related proteins with guanine nucleotide exchange activity. J. Cell Sci. 115, 4901–4913.

Da Silva, J.S., Dotti, C.G., 2002. Breaking the neuronal sphere: regulation of the actin cytoskeleton in neuritogenesis. Nat. Rev. Neurosci. 3, 694–704.

Dasso, M., 2001. Running on Ran: nuclear transport and the mitotic spindle. Cell 104, 321–324.

Delprato, A., Merithew, E., Lambright, D.G., 2004. Structure, exchange determinants, and family-wide rab specificity of the tandem helical bundle and Vps9 domains of Rabex-5. Cell 118, 607–617.

Devon, R.S., Orban, P.C., Gerrow, K., Barbieri, M.A., Schwab, C., Cao, L.P., Helm, J.R., Bissada, N., Cruz-Aguado, R., Davidson, T.L., Witmer, J., Metzler, M., Lam, C.K., Tetzlaff, W., Simpson, E.M., McCaffery, J.M., El-Husseini, A.E., Leavitt, B.R., Hayden, M.R., 2006. *Als2*-deficient mice exhibit disturbances in endosome trafficking associated with motor behavioral abnormalities. Proc. Natl. Acad. Sci. U.S.A. 103, 9595–9600.

Devon, R.S., Schwab, C., Topp, J.D., Orban, P.C., Yang, Y.Z., Pape, T.D., Helm, J.R., Davidson, T.L., Rogers, D.A., Gros-Louis, F., Rouleau, G., Horazdovsky, B.F., Leavitt, B.R., Hayden, M.R., 2005. Cross-species characterization of the *ALS2* gene and analysis of its pattern of expression in development and adulthood. Neurobiol. Dis. 18, 243–257.

Devon, R.S., Helm, J.R., Rouleau, G.A., Leitner, Y., Lerman-Sagie, T., Lev, D., Hayden, M.R., 2003. The first nonsense mutation in alsin results in a homogeneous phenotype of infantile-onset ascending spastic paralysis with bulbar involvement in two siblings. Clin. Genet. 64, 210–215.

Erie, E.A., Shim, H., Smith, A.L., Lin, X., Keyvanfar, K., Xie, C., Chen, J., Cai, H., 2007. Mice deficient in the *ALS2* gene exhibit lymphopenia and abnormal hematopietic function. J. Neuroimmunol. 182, 226–231.

Etienne-Manneville, S., Hall, A., 2002. Rho GTPases in cell biology. Nature 420, 629–635.

Evans, K., Keller, C., Pavur, K., Glasgow, K., Conn, B., Lauring, B., 2006. Interaction of two hereditary spastic paraplegia gene products, spastin and atlastin, suggests a common pathway for axonal maintenance. Proc. Natl. Acad. Sci. U.S.A. 103, 10666–10671.

Eymard-Pierre, E., Yamanaka, K., Haeussler, M., Kress, W., Gauthier-Barichard, F., Combes, P., Cleveland, D.W., Boespflug-Tanguy, O., 2006. Novel missense mutation in *ALS2* gene results in infantile ascending hereditary spastic paralysis. Ann. Neurol. 59, 976–980.

Eymard-Pierre, E., Lesca, G., Dollet, S., Santorelli, F.M., di Capua, M., Bertini, E., Boespflug-Tanguy, O., 2002. Infantile-onset ascending hereditary spastic paralysis is associated with mutations in the alsin gene. Am. J. Hum. Genet. 71, 518–527.

Fink, J.K., 2001. Progressive spastic paraparesis: hereditary spastic paraplegia and its relation to primary and amyotrophic lateral sclerosis. Semin. Neuol. 21, 199–207.

Goytain, A., Hines, R.M., El-Husseini, A., Quamme, G.A., 2007. *NIPA1(SPG6)*, the basis for autosomal dominant form of hereditary spastic paraplegia, encodes a functional Mg^{2+} transporter. J. Biol. Chem. 282, 8060–8068.

Grbovic, O.M., Mathews, P.M., Jiang, Y., Schmidt, S.D., Dinakar, R., Summers-Terio, N.B., Ceresa, B.P., Nixon, R.A., Cataldo, A.M., 2003. Rab5-stimulated up-regulation of the endocytic pathway increases intracellular β-cleaved amyloid precursor protein carboxyl-terminal fragment levels and Aβ production. J. Biol. Chem. 278, 31261–31268.

Gros-Louis, F., Gaspar, C., Rouleau, G.A., 2006. Genetics of familial and sporadic amyotrophic lateral sclerosis. Biochim. Biophys. Acta 1762, 956–972.

Gros-Louis, F., Meijer, I.A., Hand, C.K., Dube, M.P., MacGregor, D.L., Seni, M.H., Devon, R.S., Hayden, M.R., Andermann, F., Andermann, E., Rouleau, G.A., 2003. An *ALS2* gene mutation causes hereditary spastic paraplegia in a Pakistani kindred. Ann. Neurol. 53, 144–145.

Hadano, S., Benn, S.C., Kakuta, S., Otomo, A., Sudo, K., Kunita, R., Suzuki-Utsunomiya, K., Mizumura, H., Shefner, J.M., Cox, G.A., Iwakura, Y., Brown Jr., R.H., Ikeda, J.-E., 2006. Mice deficient in the Rab5 guanine nucleotide exchange factor ALS2/alsin exhibit age-dependent neurological deficits and altered endosome trafficking. Hum. Mol. Genet. 15, 233–250.

Hadano, S., Ikeda, J.-E., 2005. Purification and functional analyses of ALS2 and its homologue. Methods Enzymol. 403, 310–321.

Hadano, S., Otomo, A., Suzuki-Utsunomiya, K., Kunita, R., Yanagisawa, Y., Showguchi-Miyata, J., Mizumura, H., Ikeda, J.-E., 2004. ALS2CL, the novel protein highly homologous to the carboxy-terminal half of ALS2, binds to Rab5 and modulates endosome dynamics. FEBS Lett. 575, 64–70.

Hadano, S., Hand, C.K., Osuga, H., Yanagisawa, Y., Otomo, A., Devon, R.S., Miyamoto, N., Showguchi-Miyata, J., Okada, Y., Singaraja, R., Figlewicz, D.A., Kwiatkowski, T., Hosler, B.A., Sagie, T., Skaug, J., Nasir, J., Brown Jr., R.H., Scherer, S.W., Rouleau, G.A., Hayden, M.R., Ikeda, J.-E., 2001a. A gene encoding a putative GTPase regulator is mutated in familial amyotrophic lateral sclerosis 2. Nat. Genet. 29, 166–173.

Hadano, S., Yanagisawa, Y., Skaug, J., Fichter, K., Nasir, J., Martindale, D., Koop, B.F., Scherer, S.W., Nicholson, D.W., Rouleau, G.A., Ikeda, J.-E., Hayden, M.R., 2001b. Cloning and characterization of three novel genes, *ALS2CR1*, *ALS2CR2*, and *ALS2CR3*, in the juvenile amyotrophic lateral sclerosis (ALS2) critical region at chromosome 2q33–q34: candidate genes for ALS2. Genomics 71, 200–213.

Hadano, S., Nichol, K., Brinkman, R.R., Nasir, J., Martindale, D., Koop, B.F., Nicholson, D.W., Scherer, S.W., Ikeda, J.-E., Hayden, M.R., 1999. A yeast artificial chromosome-based physical map of the juvenile amyotrophic lateral sclerosis (ALS2) critical region on human chromosome 2q33–q34. Genomics 55, 106–112.

Hand, C.K., Devon, R.S., Gros-Louis, F., Rochefort, D., Khoris, J., Meininger, V., Bouchard, J.P., Camu, W., Hayden, M.R., Rouleau, G.A., 2003. Mutation screening of the *ALS2* gene in sporadic and familial amyotrophic lateral sclerosis. Arch. Neurol. 60, 1768–1771.

Hentati, A., Bejaoui, K., Pericak-Vance, M.A., Hentati, F., Speer, M.C., Hung, W.Y., Figlewicz, D.A., Haines, J., Rimmler, J., Ben Hamida, C.B., Hamida, M.B., Brown Jr., R.H., Siddique, T., 1994. Linkage of recessive familial amyotrophic lateral sclerosis to chromosome 2q33–q35. Nat. Genet. 7, 425–428.

Hirai, H., 2001. Modification of AMPA receptor clustering regulates cerebellar synaptic plasticity. Neurosci. Res. 39, 261–267.

Hosler, B.A., Sapp, P.C., Berger, R., O'Neill, G., Bejaoui, K., Hamida, M.B., Hentati, F., Chin, W., McKenna-Yasek, D., Haines, J.L., Patterson, D., Horvitz, H.R., Brown Jr., R.H., Day, C.B., 1998. Refined mapping and characterization of the recessive familial amyotrophic lateral sclerosis locus (ALS2) on chromosome 2q33. Neurogenetics 2, 34–42.

Jacquier, A., Buhler, E., Schafer, M.K., Bohl, D., Blanchard, S., Beclin, C., Haase, G., 2006. Alsin/Rac1 signaling controls survival and growth of spinal motoneurons. Ann. Neurol. 60, 105–117.

James, P.A., Talbot, K., 2006. The molecular genetics of non-ALS motor neuron diseases. Biochim. Biophys. Acta 1762, 986–1000.

Julien, J.P., Kriz, J., 2006. Transgenic mouse models of amyotrophic lateral sclerosis. Biochim. Biophys. Acta 1762, 1013–1024.

Kanekura, K., Nishimoto, I., Aiso, S., Matsuoka, M., 2006. Characterization of amyotrophic lateral sclerosis-linked P56S mutation of vesicle-associated membrane protein-associated protein B (VAPB/ALS8). J. Biol. Chem. 281, 30223–30233.

Kanekura, K., Hashimoto, Y., Kita, Y., Sasabe, J., Aiso, S., Nishimoto, I., Matsuoka, M., 2005. A Rac1/phosphatidylinositol 3-kinase/Akt3 anti-apoptotic pathway, triggered by AlsinLF, the product of the ALS2 gene, antagonizes Cu/Zn-superoxide dismutase (SOD1) mutant-induced motoneuronal cell death. J. Biol. Chem. 280, 4532–4543.

Kanekura, K., Hashimoto, Y., Niikura, T., Aiso, S., Matsuoka, M., Nishimoto, I., 2004. Alsin, the product of *ALS2* gene, suppresses SOD1 mutant neurotoxicity through RhoGEF domain by interacting with SOD1 mutants. J. Biol. Chem. 279, 19247–19256.

Kawahara, Y., Ito, K., Sun, H., Aizawa, H., Kanazawa, I., Kwak, S., 2004. Glutamate receptors: RNA editing and death of motor neurons. Nature 427, 801.

Kress, J.A., Kuhnlein, P., Winter, P., Ludolph, A.C., Kassubek, J., Muller, U., Sperfeld, A.D., 2005. Novel mutation in the *ALS2* gene in juvenile amyotrophic lateral sclerosis. Ann. Neurol. 58, 800–803.

Kunita, R., Otomo, A., Mizumura, H., Suzuki-Utsunomiya, K., Hadano, S., Ikeda, J.-E., 2007. The Rab5 activator ALS2/alsin acts as a novel Rac1 effector through Rac1-activated endocytosis. J. Biol. Chem. 282, 16599–16611.

Kunita, R., Otomo, A., Mizumura, H., Suzuki, K., Showguchi-Miyata, J., Yanagisawa, Y., Hadano, S., Ikeda, J.-E., 2004. Homo-oligomerization of ALS2 through its unique carboxyl-terminal regions is essential for the ALS2-associated Rab5 guanine nucleotide exchange activity and its regulatory function on endosome trafficking. J. Biol. Chem. 279, 38626–38635.

Kwak, S., Weiss, J.H., 2006. Calcium-permeable AMPA channels in neurodegenerative disease and ischemia. Curr. Opin. Neurobiol. 16, 281–287.

Lai, C., Xie, C., McCormack, S.G., Chiang, H.C., Michalak, M.K., Lin, X., Chandran, J., Shim, H., Shimoji, M., Cookson, M.R., Huganir, R.L., Rothstein, J.D., Price, D.L., Wong, P.C., Martin, L.J., Zhu, J.J., Cai, H., 2006. Amyotrophic lateral sclerosis 2-deficiency leads to neuronal degeneration in amyotrophic lateral sclerosis through altered AMPA receptor trafficking. J. Neurosci. 26, 11798–11806.

Lein, E.S., Hawrylycz, M.J., Ao, N., Ayres, M., Bensinger, A., Bernard, A., Boe, A.F., Boguski, M.S., Brockway, K.S., Byrnes, E.J., Chen, L., Chen, L., Chen, T.M., Chin, M.C., Chong, J., Crook, B.E., Czaplinska, A., Dang, C.N., Datta, S., Dee, N.R., Desaki, A.L., Desta, T., Diep, E., Dolbeare, T.A., Donelan, M.J., Dong, H.W., Dougherty, J.G., Duncan, B.J., Ebbert, A.J., Eichele, G., Estin, L.K., Faber, C., Facer, B.A., Fields, R., Fischer, S.R., Fliss, T.P., Frensley, C., Gates, S.N., Glattfelder, K.J., Halverson, K.R., Hart, M.R., Hohmann, J.G., Howell, M.P., Jeung, D.P., Johnson, R.A., Karr, P.T., Kawal, R., Kidney, J.M., Knapik, R.H., Kuan, C.L., Lake, J.H., Laramee, A.R., Larsen, K.D., Lau, C., Lemon, T.A., Liang, A.J., Liu, Y., Luong, L.T., Michaels, J., Morgan, J.J., Morgan, R.J., Mortrud, M.T., Mosqueda, N.F., Ng, L.L., Ng, R., Orta, G.J., Overly, C.C., Pak, T.H., Parry, S.E., Pathak, S.D., Pearson, O.C., Puchalski, R.B., Riley, Z.L., Rockett, H.R., Rowland, S.A., Royall, J.J., Ruiz, M.J., Sarno, N.R., Schaffnit, K., Shapovalova, N.V., Sivisay, T., Slaughterbeck, C.R., Smith, S.C., Smith, K.A., Smith, B.I., Sodt, A.J., Stewart, N.N., Stumpf, K.R., Sunkin, S.M., Sutram, M., Tam, A., Teemer, C.D., Thaller, C., Thompson, C.L., Varnam, L.R., Visel, A., Whitlock, R.M., Wohnoutka, P.E., Wolkey, C.K., Wong, V.Y., Wood, M., Yaylaoglu, M.B., Young, R.C., Youngstrom, B.L., Yuan, X.F., Zhang, B., Zwingman, T.A., Jones, A.R., 2007. Genome-wide atlas of gene expression in the adult mouse brain. Nature 445, 168–176.

Lesca, G., Eymard-Pierre, E., Santorelli, F.M., Cusmai, R., Di Capua, M., Valente, E.M., Attia-Sobol, J., Plauchu, H., Leuzzi, V., Ponzone, A., Boespflug-Tanguy, O., Bertini, E., 2003. Infantile ascending hereditary spastic paralysis (IAHSP): clinical features in 11 families. Neurology 60, 674–682.

Lin, X., Shim, H., Cai, H., 2007. Deficiency in the ALS2 gene does not affect the motor neuron degeneration in SOD1G93A transgenic mice. Neurobiol. Aging [Epub ahead of print].

Lodhi, I.J., Chiang, S.H., Chang, L., Vollenweider, D., Watson, R.T., Inoue, M., Pessin, J.E., Saltiel, A.R., 2007. Gapex-5, a Rab31 guanine nucleotide exchange factor that regulates Glut4 trafficking in adipocytes. Cell Metab. 5, 59–72.

Luo, L., 2000. Rho GTPases in neuronal morphogenesis. Nat. Rev. Neurosci. 1, 173–180.

Mannan, A.U., Krawen, P., Sauter, S.M., Boehm, J., Chronowska, A., Paulus, W., Neesen, J., Engel, W., 2006. ZFYVE27 (SPG33), a novel spastin-binding protein, is mutated in hereditary spastic paraplegia. Am. J. Hum. Genet. 79, 351–357.

Matsuoka, M., Nishimoto, I., 2005. Anti-ALS activity of alsin, the product of the *ALS2* gene, and activity-dependent neurotrophic factor. Neurodegener. Dis. 2, 135–138.

Miaczynska, M., Christoforidis, S., Giner, A., Shevchenko, A., Uttenweiler-Joseph, S., Habermann, B., Wilm, M., Parton, R.G., Zerial, M., 2004. APPL proteins link Rab5 to nuclear signal transduction via an endosomal compartment. Cell 116, 445–456.

Millecamps, S., Gentil, B.J., Gros-Louis, F., Rouleau, G., Julien, J.P., 2005. Alsin is partially associated with centrosome in human cells. Biochim. Biophys. Acta 1745, 84–100.

Nagano, I., Murakami, T., Shiote, M., Manabe, Y., Hadano, S., Yanagisawa, Y., Ikeda, J.-E., Abe, K., 2003. Single-nucleotide polymorphisms in uncoding regions of *ALS2* gene of Japanese patients with autosomal-recessive amyotrophic lateral sclerosis. Neurol. Res. 25, 505–509.

Otomo, A., Hadano, S., Okada, T., Mizumura, H., Kunita, R., Nishijima, H., Showguchi-Miyata, J., Yanagisawa, Y., Kohiki, E., Suga, E., Yasuda, M., Osuga, H., Nishimoto, T., Narumiya, S., Ikeda, J.-E., 2003. ALS2, a novel guanine nucleotide exchange factor for the small GTPase Rab5, is implicated in endosomal dynamics. Hum. Mol. Genet. 12, 1671–1687.

Pal, A., Severin, F., Lommer, B., Shevchenko, A., Zerial, M., 2006. Huntingtin-HAP40 complex is a novel Rab5 effector that regulates early endosome motility and is up-regulated in Huntington's disease. J. Cell Biol. 172, 605–618.

Panzeri, C., De Palma, C., Martinuzzi, A., Daga, A., De Polo, G., Bresolin, N., Miller, C.C., Tudor, E.L., Clementi, E., Bassi, M.T., 2006. The first *ALS2* missense mutation associated with JPLS reveals new aspects of alsin biological function. Brain 129, 1710–1719.

Pasinelli, P., Brown, R.H., 2006. Molecular biology of amyotrophic lateral sclerosis: insights from genetics. Nat. Rev. Neurosci. 7, 710–723.

Rakhit, R., Chakrabartty, A., 2006. Structure, folding, and misfolding of Cu, Zn superoxide dismutase in amyotrophic lateral sclerosis. Biochim. Biophys. Acta 1762, 1025–1037.

Rosen, D.R., Siddique, T., Patterson, D., Figlewicz, D.A., Sapp, P., Hentati, A., Donaldson, D., Goto, J., O'Regan, J.P., Deng, H.X., Rahmani, Z., Krizus, A., McKenna-Yasek, D., Cayabyab, A., Gaston, S.M., Berger, R., Tanzi, R.E., Halperin, J.J., Herzfeldt, B., Van den Bergh, R., Hung, W.Y., Bird, T., Deng, G., Mulder, D.W., Smyth, C., Laing, N.G., Soriano, E., Pericak-Vance, M.A., Haines, J., Rouleau, G.A., Gusella, J.S., Horvitz, H.R., Brown Jr., R.H., 1993. Mutation in Cu/Zn superoxide dismutase gene are associated with familial amyotrophic lateral sclerosis. Nature 362, 59–62.

Rossman, K.L., Der, C.J., Sondek, J., 2005. GEF means go: turning on Rho GTPases with guanine nucleotide-exchange factors. Nat. Rev. Mol. Cell Biol. 6, 167–180.

Shaw, P.J., 2005. Molecular and cellular pathways of neurodegeneration in motor neurone disease. J. Neurol. Neurosurg. Psychiatry 76, 1046–1057.

Shirane, M., Nakayama, K.I., 2006. Protrudin induces neurite formation by directional membrane trafficking. Science 314, 818–821.

Simpson, C.L., Al-Chalabi, A., 2006. Amyotrophic lateral sclerosis as a complex genetic disease. Biochim. Biophys. Acta 1762, 973–985.

Skibinski, G., Parkinson, N.J., Brown, J.M., Chakrabarti, L., Lloyd, S.L., Hummerich, H., Nielsen, J.E., Hodges, J.R., Spillantini, M.G., Thusgaard, T., Brandner, S., Brun, A., Rossor, M.N., Gade, A., Johannsen, P., Sorensen, S.A., Gydesen, S., Fisher, E.M., Collinge, J., 2005. Mutations in the endosomal ESCRTIII-complex subunit CHMP2B in frontotemporal dementia. Nat. Genet. 37, 806–808.

Snider, W.D., Zhou, F.-Q., Zhong, Z., Markus, A., 2002. Signaling the pathway to regeneration. Neuron 35, 13–16.

Stenmark, H., Olkkonen, V.M., 2001. The Rab GTPase family. Genome Biol. 2, 3007.1–3007.7.

Suzuki-Utsunomiya, K., Hadano, S., Otomo, A., Kunita, R., Mizumura, H., Osuga, H., Ikeda, J.-E., 2007. ALS2CL, a novel ALS2-interactor, modulates ALS2-mediated endosome dynamics. Biochem. Biophys. Res. Commun. 354, 491–497.

Takeshima, H., Komazaki, S., Nishi, M., Iino, M., Kangawa, K., 2000. Junctophilins: a novel family of junctional membrane complex proteins. Mol. Cell 6, 11–22.

Topp, J.D., Gray, N.W., Gerard, R.D., Horazdovsky, B.F., 2004. Alsin is a Rab5 and Rac1 guanine nucleotide exchange factor. J. Biol. Chem. 279, 24612–24623.

Tudor, E.L., Perkinton, M.S., Schmidt, A., Ackerley, S., Brownlees, J., Jacobsen, N.J., Byers, H.L., Ward, M., Hall, A., Leigh, P.N., Shaw, C.E., McLoughlin, D.M., Miller, C.C., 2005. ALS2/Alsin regulates Rac-PAK signaling and neurite outgrowth. J. Biol. Chem. 280, 34735–34740.

Van Aelst, L., Symons, M., 2002. Role of Rho family GTPases in epithelial morphogenesis. Genes Dev. 16, 1032–1054.

Verma, A., Bradley, W.G., 2001. Atypical motor neuron disease and related motor syndromes. Semin. Neurol. 21, 177–187.

Vetter, I.R., Wittinghofer, A., 2001. The guanine-nucleotide-binding switch in three dimensions. Science 294, 1299–1304.

Yamanaka, K., Miller, T.M., McAlonis-Downes, M., Chun, S.J., Cleveland, D.W., 2006. Progressive spinal axonal degeneration and slowness in ALS2-deficient mice. Ann. Neurol. 60, 95–104.

Yamanaka, K., Vande Velde, C., Eymard-Pierre, E., Bertini, E., Boespflug-Tanguy, O., Cleveland, D.W., 2003. Unstable mutants in the peripheral endosomal membrane component ALS2 cause early-onset motor neuron disease. Proc. Natl. Acad. Sci. U.S.A. 100, 16041–16046.

Yang, Y., Hentati, A., Deng, H.X., Dabbagh, O., Sasaki, T., Hirano, M., Hung, W.Y., Ouahchi, K., Yan, J., Azim, A.C., Cole, N., Gascon, G., Yagmour, A., Ben-Hamida, M., Pericak-Vance, M., Hentati, F., Siddique, T., 2001. The gene encoding alsin, a protein with three guanine-nucleotide exchange factor domains, is mutated in a form of recessive amyotrophic lateral sclerosis. Nat. Genet. 29, 160–165.

Zhang, X., He, X., Fu, X.Y., Chang, Z., 2006. Varp is a Rab21 guanine nucleotide exchange factor and regulates endosome dynamics. J. Cell Sci. 119, 1053–1062.

Zerial, M., McBride, H., 2001. Rab proteins as membrane organizers. Nat. Rev. Mol. Cell Biol. 2, 107–117.

doi:10.1093/brain/awm289 Brain (2008), 131, 229–239

CAG repeat size correlates to electrophysiological motor and sensory phenotypes in SBMA

Keisuke Suzuki,[1] Masahisa Katsuno,[1,2] Haruhiko Banno,[1] Yu Takeuchi,[1] Naoki Atsuta,[1] Mizuki Ito,[1] Hirohisa Watanabe,[1] Fumitada Yamashita,[1,3] Norio Hori,[1,3] Tomohiko Nakamura,[1,3] Masaaki Hirayama,[1,3] Fumiaki Tanaka[1] and Gen Sobue[1]

[1]Department of Neurology, Nagoya University Graduate School of Medicine, [2]Institute for Advanced Research, Nagoya University and [3]Central Neurophysiological Laboratories, Nagoya University Hospital, Nagoya, Japan

Correspondence to: Gen Sobue, MD, Department of Neurology, Nagoya University Graduate School of Medicine, Nagoya 466-8550, Japan
E-mail: sobueg@med.nagoya-u.ac.jp

Spinal and bulbar muscular atrophy (SBMA) is an adult-onset, lower motor neuron disease caused by an aberrant elongation of a CAG repeat in the androgen receptor (AR) gene. The main symptoms are weakness and atrophy of bulbar, facial and limb muscles, but sensory disturbances are frequently found in SBMA patients. Motor symptoms have been attributed to the accumulation of mutant AR in the nucleus of lower motor neurons, which is more profound in patients with a longer CAG repeat. We examined nerve conduction properties including F-waves in a total of 106 patients with genetically confirmed SBMA (mean age at data collection = 53.8 years; range = 31–75 years) and 85 control subjects. Motor conduction velocities (MCV), compound muscle action potentials (CMAP), sensory conduction velocities (SCV) and sensory nerve action potentials (SNAP) were significantly decreased in all nerves examined in the SBMA patients compared with that in the normal controls, indicating that axonal degeneration is the primary process in both motor and sensory nerves. More profound abnormalities were observed in the nerves of the upper limbs than in those of the lower limbs. F-waves in the median nerve were absent in 30 of 106 cases (28.3%), but no cases of absent F-waves were observed in the tibial nerve. From an analysis of the relationship between CMAPs and SNAPs, patients were identified with different electrophysiological phenotypes: motor-dominant, sensory-dominant and non-dominant phenotypes. The CAG repeat size and the age at onset were significantly different among the patients with motor- and sensory-dominant phenotypes, indicating that a longer CAG repeat is more closely linked to the motor-dominant phenotype and a shorter CAG repeat is more closely linked to the sensory-dominant phenotype. Furthermore, when we classified the patients by CAG repeat size, CMAP values showed a tendency to be decreased in patients with a longer CAG repeat ($\geq$47), while SNAPs were significantly decreased in patients with a shorter CAG repeat (<47). In addition, we found that the frequency of aggregation in the sensory neuron cytoplasm tended to inversely correlate with the CAG repeat size in the autopsy study, supporting the view that the CAG repeat size differentially correlates with motor- and sensory-dominant phenotypes. In conclusion, our results suggest that there are unequivocal electrophysiological phenotypes influenced by CAG repeat size in SBMA.

Keywords: CAG repeat; spinal and bulbar muscular atrophy; electrophysiological phenotypes; motor-dominant; sensory-dominant

Abbreviations: CMAP = compound muscle action potential; MCV = motor conduction velocity; SBMA = spinal and bulbar muscular atrophy; SCV = sensory conduction velocity; SNAP = sensory nerve action potential

Advance Access publication December 4, 2007

Introduction

Spinal and bulbar muscular atrophy (SBMA) is a hereditary lower motor neuron disease affecting adult males (Kennedy *et al.*, 1968; Sobue *et al.*, 1989, 1993; Fischbeck *et al.*, 1997). The cause of SBMA is an aberrant elongation of a CAG repeat in the androgen receptor (AR) gene. Normally, 9–36 CAGs are observed in the AR gene in normal subjects, but 38–62 CAGs are observed in SBMA patients (La Spada *et al.*, 1991; Tanaka *et al.*, 1996; Andrew *et al.*, 1997). A similar gene mutation has been detected in Huntington's

disease (HD), dentatorubral-pallidoluysian atrophy (DRPLA) and several types of spinocerebellar ataxia (Gatchel *et al.*, 2005). Since CAG is translated to glutamine, these disorders, including SBMA, are called polyglutamine diseases. In SBMA patients, there is an inverse correlation between the number of CAGs and the age at onset (Doyu *et al.*, 1992; Atsuta *et al.*, 2006). The histopathological hallmarks of this disease are an extensive loss of lower motor neurons in the spinal cord and brain stem, together with degeneration of the dorsal root ganglions (DRG) (Sobue *et al.*, 1989; Adachi *et al.*, 2005). Intranuclear accumulations of mutant AR protein in the residual motor neurons are another hallmark (Li *et al.*, 1998; Adachi *et al.*, 2005). The molecular basis for motor neuron degeneration is thought to be testosterone-dependent nuclear accumulation of the mutant AR, and androgen deprivation rescues neuronal dysfunction in animal models of SBMA (Katsuno *et al.*, 2002, 2003; Takeyama *et al.*, 2002; Chevalier-Larsen *et al.*, 2004). Androgen deprivation with a luteinizing hormone-releasing hormone (LHRH) analog also suppresses nuclear accumulation of mutant AR in the scrotal skin of SBMA patients (Banno *et al.*, 2006). Other candidates for potent therapeutics such as 17-allylamino-17-demethoxygeldanamycin (17-AAG) or geranylgeranylacetone (GGA), enhancers of molecular chaperone expression and function, and a histone deacetylase (HDAC) inhibitor have also emerged from studies of animal models of SBMA (Minamiyama *et al.*, 2004; Katsuno *et al.*, 2005; Waza *et al.*, 2005).

The main symptoms of SBMA are weakness and atrophy of the bulbar, facial and limb muscles (Katsuno *et al.*, 2006). The onset of weakness is usually between 30 and 60 years of age. Postural tremor of the fingers is often observed prior to weakness. The symptoms are slowly progressive in SBMA, and the susceptibility for aspiration pneumonia increases as bulbar paralysis develops (Atsuta *et al.*, 2006). The most common cause of death is pneumonia. Many patients also have hypertension, hyperlipidemia, liver dysfunction and glucose intolerance. Serum creatine kinase is increased in the majority of patients.

In addition to motor symptoms, sensory impairment such as vibratory sensory disorder is often observed, and electrophysiological involvement has also been described in sensory nerves of SBMA patients (Harding *et al.*, 1982; Olney *et al.*, 1991; Li *et al.*, 1995; Guidetti *et al.*, 1996; Polo *et al.*, 1996; Ferrante *et al.*, 1997; Antonini *et al.*, 2000; Sperfeld *et al.*, 2002). In addition, sensory nerve axon loss, particularly of the central and peripheral rami of primary sensory neurons, has been documented to be profound (Harding *et al.*, 1982; Sobue *et al.*, 1989; Li *et al.*, 1995). Spinal dorsal column involvement and loss of axons in the sural nerve are common pathological features (Sobue *et al.*, 1989; Li *et al.*, 1995), and abnormalities in sensory nerve conduction and sensory evoked potentials are well known features of SBMA (Kachi *et al.*, 1992). Since the sensory symptoms are not generally severe in most patients, sensory nerve involvement has not been given much attention, particularly when compared to motor symptoms. However, the involvement of primary sensory neurons is one of the major phenotypic manifestations in SBMA (Sobue *et al.*, 1989).

The age at onset and the severity of motor symptoms are variable among SBMA patients (Kennedy *et al.*, 1968; Sperfeld *et al.*, 2002). One of the major factors determining clinical features is the CAG repeat size in the AR gene (Doyu *et al.*, 1992; Atsuta *et al.*, 2006). However, the age at onset and severity are also variable even among the patients with the same CAG repeat size (Doyu *et al.*, 1992; Atsuta *et al.*, 2006), indicating that some unknown genetic or environmental factors may influence the development of clinical heterogeneity (Atsuta *et al.*, 2006). In sensory impairments, there is also a variable degree of severity. Some patients show profound sensory symptoms and sensory nerve electrophysiological abnormalities, while other patients appear almost normal (Olney *et al.*, 1991; Li *et al.*, 1995; Guidetti *et al.*, 1996; Antonini *et al.*, 2000). In contrast to motor symptoms, the age at onset for sensory symptoms is rather difficult to determine, and the role of CAG repeat size in the severity of symptoms and the onset of sensory symptoms is unknown.

In order to clarify motor and sensory nerve involvement in SBMA, we examined nerve conduction properties including F-waves in 106 patients with genetically confirmed SBMA and 85 control subjects. We further analysed the influence of the CAG repeat size within the AR gene on the electrophysiological motor- and sensory-dominancy, as well as the histopathological background underlying the phenotypic diversity in nerve conduction of SBMA patients.

Subjects and Methods

Patients

A total of 106 male patients with the diagnosis of SBMA confirmed by genetic analysis and 85 male normal control subjects were included in this study. The data of SBMA patients were collected between May 2003 and May 2007. We analysed various electrophysiological examinations, motor function, sensory disturbance, disease duration and CAG repeat size in the AR gene in these patients. We defined the onset of disease as when the muscular weakness began, but not when tremor of the fingers appeared. As a functional assessment, we applied the Limb Norris score, Norris Bulbar score and ALS functional rating scale-revised (ALSFRS-R), which are aimed at motor function evaluations of patients with amyotrophic lateral sclerosis (ALS) (Norris *et al.*, 1974; The ALS CNTF Treatment Study (ACTS) Phase I-II Study Group, 1996).

All studies conformed to the ethics guideline for human genome/gene analysis research and the ethics guideline for epidemiological studies endorsed by the Japanese government. The ethics committee of Nagoya University Graduate School of Medicine approved the study, and all SBMA patients and normal subjects gave their written informed consent to the investigation.

Electrophysiological assessments

Motor and sensory nerve conduction studies were performed in the median, ulnar, tibial and sural nerves in 106 patients during their initial clinical assessment at Nagoya University Hospital using a standard method with surface electrodes for stimulation and recording as described previously (Sobue *et al.*, 1989; Kimura, 2001*a*, *b*; Koike *et al.*, 2003; Mori *et al.*, 2005). Motor conduction was investigated in the median, ulnar and tibial nerves, recording from the abductor pollicis brevis, abductor digiti minimi and abductor hallucis brevis, respectively. The following nerve segments were used for calculating motor conduction velocities (MCV): wrist to elbow for the median nerve, wrist to distally at the elbow for the ulnar nerve, and ankle to popliteal fossa for the tibial nerve. Sensory conduction was investigated in the median, ulnar and sural nerves, using antidromic recording from ring electrodes at the second and fifth digit for the median and ulnar nerves, respectively, and bar electrodes at the ankle for the sural nerve. Sensory conduction velocities (SCV) were calculated for the distal segment. Amplitudes of compound muscle action potentials (CMAP) and those of sensory nerve action potentials (SNAP) were measured from the baseline to the first negative peak. Control values were obtained in 56–85 age-matched normal volunteers (31–75 years) (Koike *et al.*, 2001; Mori *et al.*, 2005).

F-waves were also examined in the median and tibial nerves at the same time as the nerve conduction studies using a standard method as described previously (Kimura, 2001*c*). Sixteen consecutive supramaximal stimuli with frequency of 1 Hz were delivered to the median and tibial nerves, while recording from the same muscles as the normal nerve conduction studies. The following variables were estimated: occurrence, minimum latency and maximum F-wave conduction velocity (FWCV). FWCV was calculated using the formula $2D/(F-M-1)$, where D is the surface distance measured from the stimulus point to the C7 spinous process in the median nerves or to the T12 spinous process in the tibial nerves, F is the latency of the F-wave and M is the latency of the CMAP. Control values were obtained in 28–47 age-matched normal volunteers (31–75 years). All nerve conduction studies and F-wave studies were carried out on the right side of the body.

We defined the nerve conduction, CMAPs and SNAPs as abnormal, when these values were less than the mean −2 SD of normal controls on the examined nerves. We also expressed the CMAP and SNAP values as the percentage of the mean values of normal controls, when we need the standardized expression of the degree of CMAP and SNAP involvement as compared to normal controls.

Standard needle electromyography (EMG) was performed using concentric needle electrodes in 93 SBMA patients, with the muscles at rest and during weak and maximal efforts (Sobue *et al.*, 1993; Kimura, 2001*d*; Sone *et al.*, 2005).

Genetic analysis

Genomic DNA was extracted from peripheral blood of SBMA patients using conventional techniques (Tanaka *et al.*, 1996). PCR amplification of the CAG repeat in the AR gene was performed using a fluorescein-labelled forward primer (5′-TCC AGAATCTGTTCCAGAGCGTGC-3′) and a non-labelled reverse primer (5′-TGGCCTCGCTCAGGATGTCTTTAAG-3′). Detailed PCR conditions were described previously (Tanaka *et al.*, 1996, 1999). Aliquots of PCR products were combined with loading dye and separated by electrophoresis with an autoread sequencer SQ-5500 (Hitachi Electronics Engineering, Tokyo, Japan). The size of the CAG repeat was analysed on Fraglys software version 2.2 (Hitachi Electronics Engineering) by comparison to co-electrophoresed PCR standards with known repeat sizes. The CAG repeat size of the PCR standard was determined by direct sequence as described previously (Doyu *et al.*, 1992).

Immunohistochemistry for mutant AR in the sensory and motor neurons

For immunohistochemistry of primary sensory and spinal motor neurons, autopsy specimens of lumbar DRG and spinal cord from five genetically diagnosed SBMA patients (70.4 ± 11.0 years old) were used. The lumbar DRG and spinal cord were excised at autopsy and immediately fixed in 10% buffered formalin solution. The collection of tissues and their use for this study were approved by the Ethics Committee of Nagoya University Graduate School of Medicine. Lumbar DRG and spinal cord sections of 6 μm were deparaffinized, treated with 98% formic acid at room temperature for 3 min and with microwave oven heating for 10 min in 10 mM citrate buffer at pH 6.0, and incubated with an anti-polyglutamine antibody (1C2, 1:20 000; Chemicon, Temecula, CA). Subsequent staining procedures are performed using the Envision+ kit (Dako, Glostrup, Denmark).

For quantification of primary sensory neurons in which mutant AR accumulates, we prepared at least 100 transverse sections from the lumbar DRG, and performed 1C2 immunohistochemistry as described above. The frequency of 1C2-positive and -negative cells within the DRG was assessed by counting all the neurons with 1C2-positive cytoplasmic inclusions against total neuronal cells with obvious nuclei on every 10th section under the light microscope (BX51N-34, Olympas, Tokyo, Japan). The results were expressed as frequency of 1C2-positive cells in the 10 sections of the DRG. As for quantification of spinal motor neurons, the detailed procedure has been described previously (Adachi *et al.*, 2005). We have also examined five control autopsied specimens from patients died from non-neurological diseases, and found that there were no 1C2-positive cytoplasmic or nuclear staining.

Data analysis

Quantitative data was presented as means ± SD. Statistical comparisons were performed using the Student's t-test. Correlations among the parameters were analysed using Pearson's correlation coefficient. P values less than 0.05 and correlation coefficients (r) greater than 0.4 were considered to indicate significance. Calculations were performed using the statistical software package SPSS 14.0J (SPSS Japan Inc., Tokyo, Japan).

Results

Clinical and genetic backgrounds of SBMA patients

The clinical background of the SBMA patients is described in Table 1. All of the patients examined were of Japanese nationality. The duration from onset assessed from the first notice of motor impairment (Atsuta *et al.*, 2006) ranged from 1 to 32 years. There was no significant difference between the median CAG repeat size in the present study

Table 1 Clinical and genetic features of SBMA patients

Clinical and genetic features	Mean ± SD	Range	*n*
Age at examination (years)	53.8 ± 10.0	31–75	106
Duration from onset (years)	10.1 ± 6.8	1–32	106
Age at onset (years)	43.7 ± 10.4	25–68	106
CAG repeat size in AR gene (number)	47.8 ± 3.1	41–57	97[a]
Limb Norris score (normal score = 63)	53.9 ± 7.3	34–63	99
Norris Bulbar score (normal score = 39)	33.0 ± 4.3	20–39	99
ALSFRS-R (normal score = 48)	41.1 ± 4.3	22–48	99

[a]The abnormal elongation of the CAG repeat was confirmed by gene analysis using agarose gel electrophoresis without determining the repeat number in the remaining nine patients. AR = androgen receptor; ALSFRS-R = ALS functional rating scale-revised

and those reported previously in SBMA patients (La Spada *et al.*, 1991; Tanaka *et al.*, 1996; Andrew *et al.*, 1997).

All patients were ambulatory with or without aid, and none were bed-ridden. The mean Limb Norris score, Norris Bulbar score and ALSFRS-R also suggested that the ADL of patients in this study was not severely impaired. Vibratory sensation disturbance was detected in 78.2% of the SBMA patients. Touch and pain sensation abnormalities were found in 10.9 and 9.1% of the patients, respectively. Joint position sensation was intact in all of the patients examined.

In EMG, all the examined patients showed high amplitude potentials, reduced interference and polyphasic potentials, suggesting neurogenic changes in SBMA.

Nerve conduction and F-wave studies indicate CMAP and SNAP reduction as a profound feature of SBMA

MCV, CMAP, SCV and SNAP were significantly decreased in all the nerves examined in the SBMA patients when compared with those of the normal controls (Table 2). Sensory nerve activity could not be evoked in some cases, whereas activity in the motor nerves was elicited in all patients examined. The most profound finding in the nerve conduction studies was the reduction in the amplitude of the evoked potentials in both motor and sensory nerves. The mean values of CMAPs were reduced to 47–76%, and SNAPs were reduced to 31–47% of the normal mean values. The decrease in conduction velocity was relatively mild, but definitely present in both motor and sensory nerves. The conduction velocity was reduced to 94–96% in MCV and 87–91% in SCV of the normal mean values. The F-wave latencies were also mildly, but significantly prolonged in the median and tibial nerves of SBMA patients. The mean occurrence rate of F-waves in the median nerve was significantly less in SBMA patients, and they were absent in 30 cases (28.3%) (Table 2).

When we compared the CMAP and MCV values of the individual patients in the median, ulnar and tibial nerves, MCV was decreased only in the patients with a severely decreased CMAP (Supplementary Fig. 1). In addition, SCV reduction was observed only in the patients with severely decreased SNAP (Supplementary Fig. 1). These observations strongly suggest that the most profound impairment of the SBMA patients is a reduction of the amplitude of evoked potentials, possibly due to axonal loss (Sobue *et al.*, 1989; Li *et al.*, 1995).

As for the spatial distribution of electrophysiological involvements, the frequency of abnormal values of CMAP was most remarkable in the median nerve followed by the ulnar and tibial nerves (Table 3). The decrease in SNAP was also remarkable in the median and ulnar nerves when compared with those in the sural nerve (Table 3). The absence of F-waves was more frequent in the median nerve than in the tibial nerve (Table 3). These findings indicate that more significant abnormalities in nerve conduction and F-waves are observed in the nerves of the upper limbs than in those of the lower limbs.

Electrophysiologically defined motor and sensory phenotypes

When we analysed the relationship between the degree of motor and sensory nerve involvement by assessing the number of nerves showing abnormally reduced amplitudes (less than control mean − 2 SD) in the sensory (median, ulnar and sural nerves) and motor (median, ulnar and tibial nerves) nerves, we found that the patients could be distinguished by either a motor-dominant, sensory-dominant or non-dominant phenotype (Fig. 1A). It should be noted that there were patients showing only abnormally reduced SNAPs, while the CMAPs were well preserved (Fig. 1A). Alternatively, patients demonstrating CMAPs abnormalities with well preserved SNAPs were also seen (Fig. 1A).

When we analysed the relationship between CMAPs and SNAPs on a standardized scale of percentage of the mean values of normal controls in the median and ulnar nerves (Fig. 1B and C), we found that there were patients with different electrophysiological phenotypes. Some patients showed well preserved CMAPs, being 50% or more of the mean value in the controls, while showing profoundly reduced SNAPs of less than 50% of the mean value in the controls. In contrast, other patients showed well-preserved SNAPs and significantly reduced CMAPs (Fig. 1B and C). Finally, some patients showed a similar involvement of CMAPs and SNAPs. These observations suggest that a subset of SBMA patients shows predominantly motor impairments, while another subset shows predominantly sensory impairments.

The CAG repeat size correlates to electrophysiologically defined motor and sensory phenotypes

Since the CAG repeat size is a key factor dictating clinical presentation in polyglutamine diseases (Zoghbi *et al.*, 2000),

Table 2 Nerve conduction studies and F-wave examinations

	SBMA		Normal		*P*
	(Mean ± SD)	*n*	(Mean ± SD)	*n*	
Median nerve					
MCV (m/s)	54.3 ± 6.5	106	57.9 ± 3.6	79	<0.001
Distal latency (m/s)	4.3 ± 1.0	106	3.4 ± 0.4	79	<0.001
CMAP (mV)	5.1 ± 2.9	106	10.8 ± 3.3	79	<0.001
SCV (m/s)	52.3 ± 6.1	103	57.4 ± 4.4	85	<0.001
SNAP (μV)	7.0 ± 5.2	103	20.0 ± 7.9	85	<0.001
Not evoked	Three cases (2.8%)		None		
F-wave minimum latency (ms)	28.2 ± 3.0	76	22.3 ± 1.9	46	<0.001
FWCV maximum (m/s)	58.7 ± 10.5	74	66.4 ± 8.6	41	<0.001
F-wave occurrence (%)	24.5 ± 22.5	106	67.6 ± 20.3	47	<0.001
Absent	30 cases (28.3%)		None		
Ulnar nerve					
MCV (m/s)	55.9 ± 5.2	106	58.2 ± 4.7	71	0.003
Distal latency (ms)	3.2 ± 0.6	106	2.7 ± 0.3	71	<0.001
CMAP (mV)	5.1 ± 2.4	106	8.4 ± 2.4	71	<0.001
SCV (m/s)	48.1 ± 7.5	102	55.0 ± 3.8	74	<0.001
SNAP (μV)	5.6 ± 4.6	102	18.3 ± 7.4	74	<0.001
Not evoked	Four cases (3.8%)		None		
Tibial nerve					
MCV (m/s)	44.5 ± 3.8	106	47.2 ± 3.7	56	<0.001
Distal latency (ms)	5.0 ± 1.0	106	4.5 ± 0.8	56	0.003
CMAP (mV)	7.8 ± 3.7	106	10.3 ± 3.4	56	<0.001
F-wave minimum latency (ms)	48.3 ± 4.1	106	41.4 ± 3.0	31	<0.001
FWCV maximum (ms)	43.9 ± 5.6	105	47.4 ± 3.3	28	<0.001
F-wave occurrence (%)	94.3 ± 11.6	106	96.3 ± 12.5	31	NS
Absent	None		None		
Sural nerve					
SCV (m/s)	44.1 ± 5.7	94	50.8 ± 5.1	68	<0.001
SNAP (μV)	5.1 ± 3.5	94	10.8 ± 4.6	68	<0.001
Not evoked	12 cases (11.3%)		None		

MCV = motor nerve conduction velocity; CMAP = compound muscle action potential; SCV = sensory nerve conduction velocity; SNAP = sensory nerve action potential; FWCV = F-wave conduction velocity; NS = not significant.

Table 3 Frequency of patients with abnormal values in nerve conduction studies and F-wave examinations

	Number of patients with abnormal values[a]	*n*	Frequency (%)
Median nerve			
MCV	20	106	18.9
CMAP	43	106	40.6
SCV	23	106	21.7
SNAP	45	106	42.5
FWCV maximum	38	104	36.5
F-wave occurrence	91	106	85.8
Ulnar nerve			
MCV	5	106	4.7
CMAP	24	106	22.6
SCV	40	106	37.7
SNAP	49	106	46.2
Tibial nerve			
MCV	6	106	5.7
CMAP	8	106	7.5
FWCV maximum	17	105	16.2
F-wave occurrence	7	106	6.6
Sural nerve			
SCV	36	106	34.0
SNAP	26	106	24.5

MCV = motor nerve conduction velocity; CMAP = compound muscle action potential; SCV = sensory nerve conduction velocity; SNAP = sensory nerve action potential; FWCV = F-wave conduction velocity.

[a]We defined the abnormal values as those values that were either less than the mean − 2 SD of normal controls on the examined nerves or not evoked.

we compared the phenotypes based on present symptoms and the electrophysiological phenotypes between patients with a CAG repeat size <47 and those with 47 or more CAGs, according to the previous report on clinical features of SBMA (Atsuta *et al.*, 2006) (Table 4). The age at onset and the age at examination were higher in patients with a shorter CAG repeat than in those with a longer repeat ($P<0.001$). Disease duration and functional scale, including the Limb Norris score, Norris Bulbar score and ALSFRS-R, were similar between these groups. The CMAP values in the median, ulnar and tibial nerves were not significantly different, but showed a tendency to be decreased in the patients with a longer CAG repeat in all three nerves (Table 4). SNAPs in the median, ulnar and sural nerves were all significantly decreased in the patients with a shorter CAG repeat (Table 4). These observations suggest that a shorter CAG repeat is linked to a more significant SNAP decrease, while a longer CAG repeat is linked to a more profound CMAP decrease.

Furthermore, considering the possibility that action potentials are influenced by the age at examination, we compared the CMAPs and SNAPs in the patient subsets with a longer CAG repeat and those with a shorter CAG repeat between different age groups (Fig. 2). Patients <49 years old showed a significant difference in CMAPs and SNAPs ($P=0.041-0.002$). The patients <49 years old and with a longer CAG repeat showed a more significant decrease in CMAPs, while those with a shorter CAG repeat showed a more significant decrease in SNAPs.

We selected patients with the sensory-dominant phenotype and those with the motor-dominant phenotype to further analyse the implication of CAG repeat size on the age at onset and electrophysiological phenotypes of SBMA.

A

Number of nerves with abnormally reduced SNAPs	Number of nerves with abnormally reduced CMAPs: 0	1	2	3
0	22	16	4	1
1	11	6	3	2
2	12	9	2	2
3	10	2	3	1

Motor-dominant
Sensory-dominant
Non-dominant

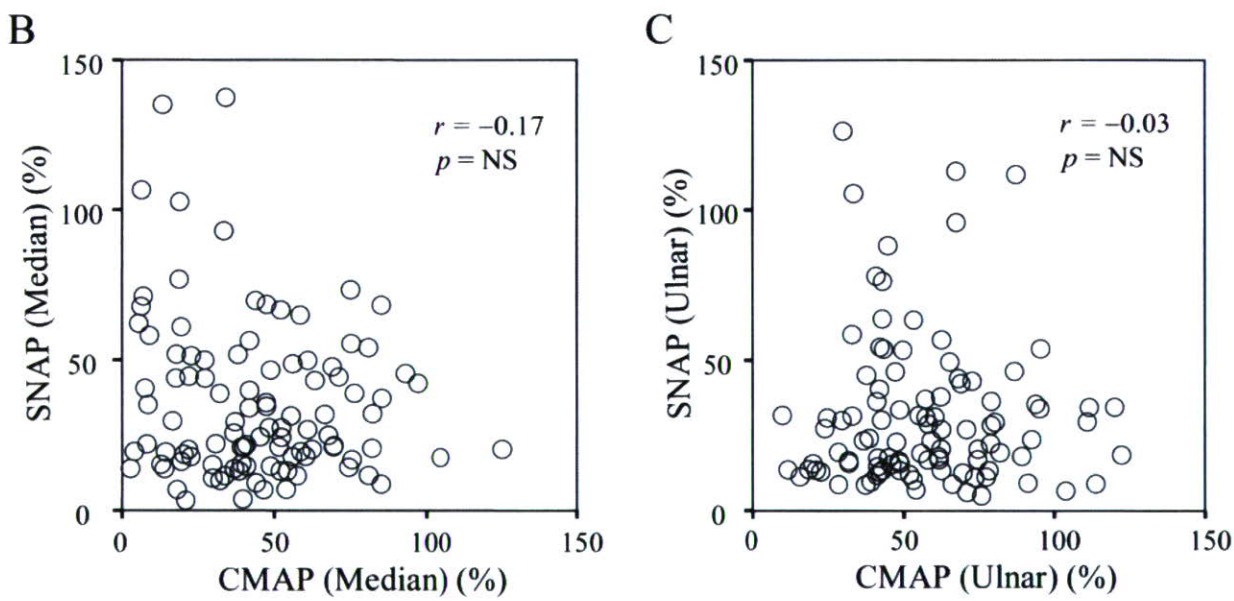

Fig. 1 Electrophysiological discrepancies in motor and sensory nerve involvement in SBMA patients. (**A**) The cross tabulation of the number of motor and sensory nerves showing an abnormally decreased action potential. The vertical stripe area corresponds to the motor-dominant phenotype and the gray area denotes the sensory-dominant phenotype. The white area represents the non-dominant phenotype. (**B** and **C**). Relation between CMAP and SNAP in the median and ulnar nerves on a standardized scale of percentage to normal control mean values. Some patients have only decreases of CMAP with preserved SNAP, while other patients show declines of SNAP with conserved CMAP.

As shown in Fig. 1A, the sensory-dominant phenotype was determined if patients show a reduced SNAP (less than control mean −2 SD) in at least one nerve without any decrease in CMAPs, whereas the motor-dominant phenotype denotes patients showing a reduced CMAP (less than control mean −2 SD) in at least one nerve without any decrease in SNAPs. We examined the relationship between CAG repeat number and the age at onset in these patients ($n=54$) (Fig. 3A). We found that the mean CAG repeat number and the age at onset were significantly different between patients with motor- and sensory-dominant phenotypes ($P<0.001$, Fig. 3A), indicating that a longer CAG repeat is more closely linked to the motor-dominant phenotype, and a shorter CAG repeat is more closely linked to sensory-dominant phenotype. Similar findings were observed when we classified patients based on abnormally reduced action potentials (less than control mean −2 SD) in the median nerve or the ulnar nerve (Fig. 3B and C).

Table 4 Clinical and electrophysiological features in terms of CAG repeat size in AR gene

	CAG repeat <47		CAG repeat ⩾47		*P*
	(Mean ± SD)	*n*	(Mean ± SD)	*n*	
Age at examination	58.9 ± 10.2	32	51.7 ± 8.9	65	0.001
Duration from onset	9.6 ± 7.4	32	10.7 ± 6.6	65	NS
Age at onset	49.3 ± 11.5	32	41.0 ± 8.9	65	0.002
Limb Norris score	54.2 ± 8.3	28	53.9 ± 7.0	63	NS
Norris Bulbar score	32.4 ± 5.1	28	33.4 ± 3.9	63	NS
ALSFRS-R	41.1 ± 4.1	28	41.2 ± 4.5	63	NS
CMAP (mV)					
Median	5.7 ± 2.4	32	4.8 ± 3.1	65	NS
Ulnar	5.6 ± 2.2	32	4.9 ± 2.4	65	NS
Tibial	8.7 ± 4.9	32	7.4 ± 3.1	65	NS
SNAP (μV)					
Median	4.8 ± 3.3	29	7.7 ± 5.6	65	0.011
Ulnar	4.1 ± 2.6	29	6.2 ± 5.0	64	0.037
Sural	3.8 ± 2.6	26	5.4 ± 3.4	59	0.022

AR = androgen receptor; ALSFRS-R = ALS functional rating scale-revised; CAMP = compound muscle action potential; SNAP = sensory nerve action potential; NS = not significant.

The CAG repeat size correlates directly with the frequency of nuclear accumulation in the motor neurons and inversely with that of cytoplasmic aggregation in the DRG

In order to investigate the relationship between CAG repeat size and the degree of motor and sensory nerve involvement, we performed immunohistochemistry using anti-polyglutamine antibody (1C2) on autopsied spinal cord and DRG specimens from SBMA patients, and quantified the primary sensory neurons in which mutant AR accumulated. In primary sensory neurons within the DRG, mutant AR was detected immunochistochemically as punctuate aggregates in the cytoplasm (Fig. 4A). On the other hand, diffuse nuclear accumulation of mutant AR was detected in motor neurons of the spinal anterior horn (Fig. 4B). The size of CAG repeat in the AR gene tended to be inversely correlated with the number of primary sensory neurons bearing cytoplasmic aggregates (Fig. 4C). This result is in contrast with the previously reported correlation between the frequency of mutant AR accumulation in spinal motor neuron and the CAG repeat size (Adachi *et al.*, 2005) (Fig. 4D).

Discussion

The present study demonstrated extensive abnormalities in both motor and sensory nerve conduction in SBMA patients, reflecting principal pathological lesions in the lower motor neurons and in the DRG. Previous studies on nerve conduction in SBMA patients showed a characteristic decrease in SNAP compared with normal controls, whereas SCV and MCV were variably reported as either normal or decreased, and CMAP decreased to variable extents (Harding *et al.*, 1982; Olney *et al.*, 1991; Li *et al.*, 1995; Guidetti *et al.*, 1996; Polo *et al.*, 1996; Ferrante *et al.*, 1997; Antonini *et al.*, 2000; Sperfeld *et al.*, 2002). In the present study, the reductions in both CMAP and SNAP were remarkable, in agreement with previous reports. This suggests that axonal degeneration is the principal peripheral nerve damage in SBMA patients. In addition, MCVs and SCVs were significantly decreased in the SBMA patients, and distal latencies were also significantly increased.

Several reports have examined the F-wave in SBMA patients. Those studies showed that the latency is almost normal or slightly extended (Olney *et al.*, 1991; Guidetti *et al.*, 1996). In the present study, the minimum F-wave latency was significantly longer and the maximum FWCV was significantly decreased in SBMA patients compared to that in normal controls. The occurrence of F-waves in SBMA patients was significantly less in the upper limb, but not in the lower limb compared with that of controls.

As for the spatial distribution of involvement, we demonstrated that nerves of the upper limbs are more severely disturbed than those of the lower limbs in SBMA patients. These observations suggest that nerve involvement does not reflect a length-dependent process of primary neuropathy, but a neuronopathy process, which is consistent with our results from histopathological studies (Sobue *et al.*, 1989; Li *et al.*, 1995).

The most striking observations in the present study are that motor and sensory nerves are differentially affected in SBMA patients, that electrophysiologically defined motor-dominant and sensory-dominant phenotypes are present, especially in young patients, and that the CAG repeat size in the AR gene is a factor determining these electrophysiologically defined motor and sensory phenotypes. Previous studies have reported that the number of CAGs determine not only the age at onset, but also the clinical phenotype in polyglutamine diseases (Ikeutchi *et al.*, 1995; Johansson *et al.*, 1998; Mahant *et al.*, 2003). For example, DRPLA patients with a longer CAG repeat (earlier age at onset) showed a progressive myoclonus epilepsy phenotype, whereas patients with a shorter CAG repeat (later age at onset) showed a non-progressive myoclonus epilepsy phenotype, but high frequencies of choreoathetosis and psychiatric symptoms (Ikeutchi *et al.*, 1995). Moreover, in spinocerebellar ataxia type-7 (SCA7) patients with ⩾59 CAGs, visual impairment was the most common initial symptom observed, while ataxia predominated in patients with <59 CAGs (Johansson *et al.*, 1998). Additionally, in HD patients, younger age at onset was associated with less chorea and more dystonia (Mahant *et al.*, 2003). In SBMA, only the relationship between CAG repeat and the age at onset or the severity of motor

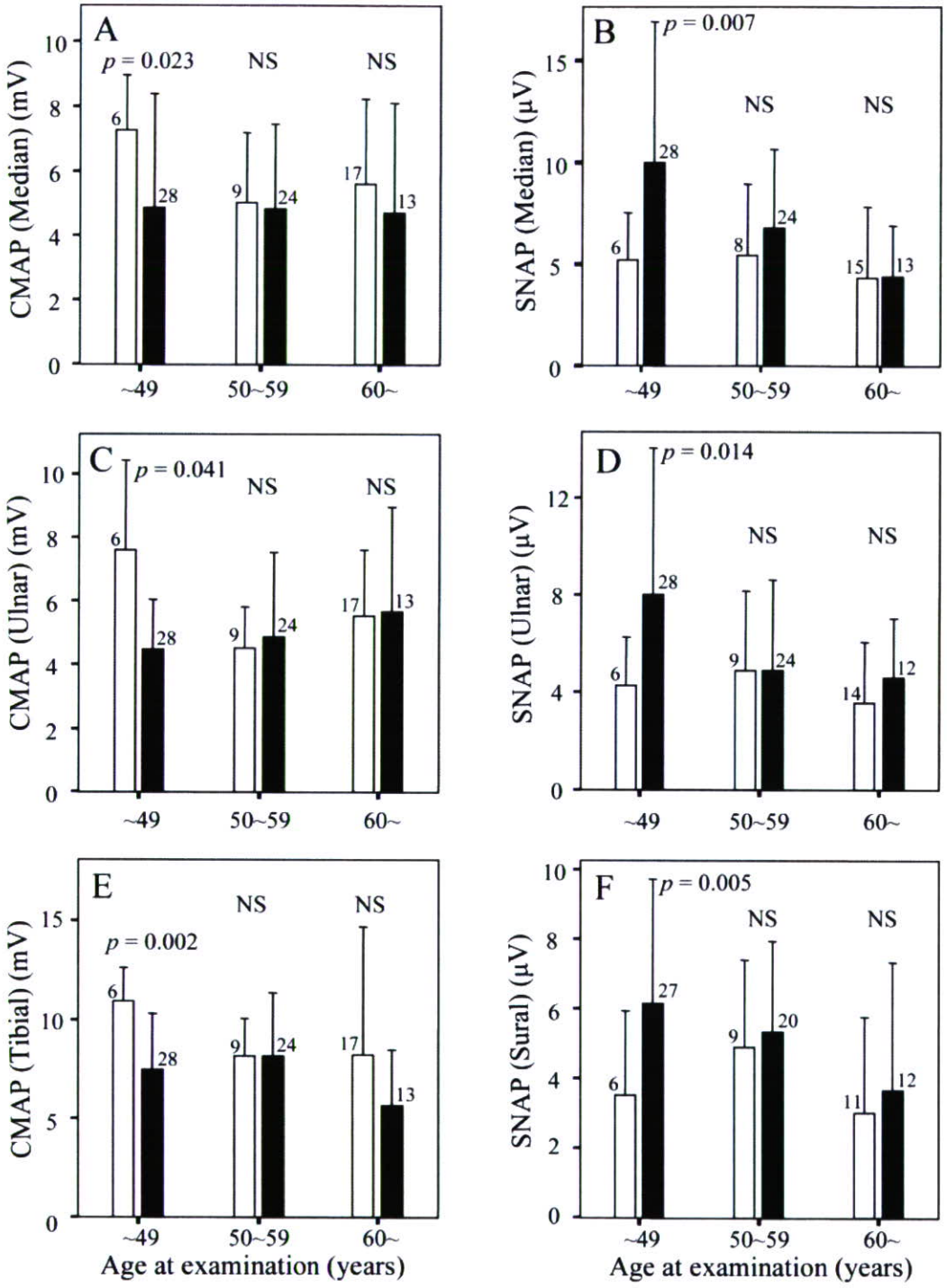

Fig. 2 (**A–F**) Age- and CAG-dependent changes in motor and sensory amplitudes in SBMA. CMAPs and SNAPs in the median (A and B), ulnar (C and D), tibial (E) and sural (F) nerves in different age groups are shown. The white columns are the mean values of the patients with a shorter CAG repeat (<47), while the black columns are the mean values of the patients with a longer CAG repeat (≥47). The error bars are SD. The number of patients examined is shown above each column. The young patients with a longer CAG repeat showed significantly low values of CMAPs compared to those with a shorter CAG repeat. Conversely, young patients with a shorter CAG repeat showed significantly lower values of SNAPs than those with a longer CAG repeat. Patients more than 49 years old did not show a significant difference between shorter and longer CAG repeat.

function has been reported (Doyu *et al.*, 1992; Atsuta *et al.*, 2006), but a CAG size-dependent clinical phenotype has not been described. This may be because the expansion of CAG repeat in the AR gene is shorter than that in the causative genes for DRPLA, SCA7 or HD. Alternatively, as compared to outstanding motor dysfunction, the clinical manifestations of sensory nerve impairment are less severe in SBMA patients, which may result in overlooking the motor and

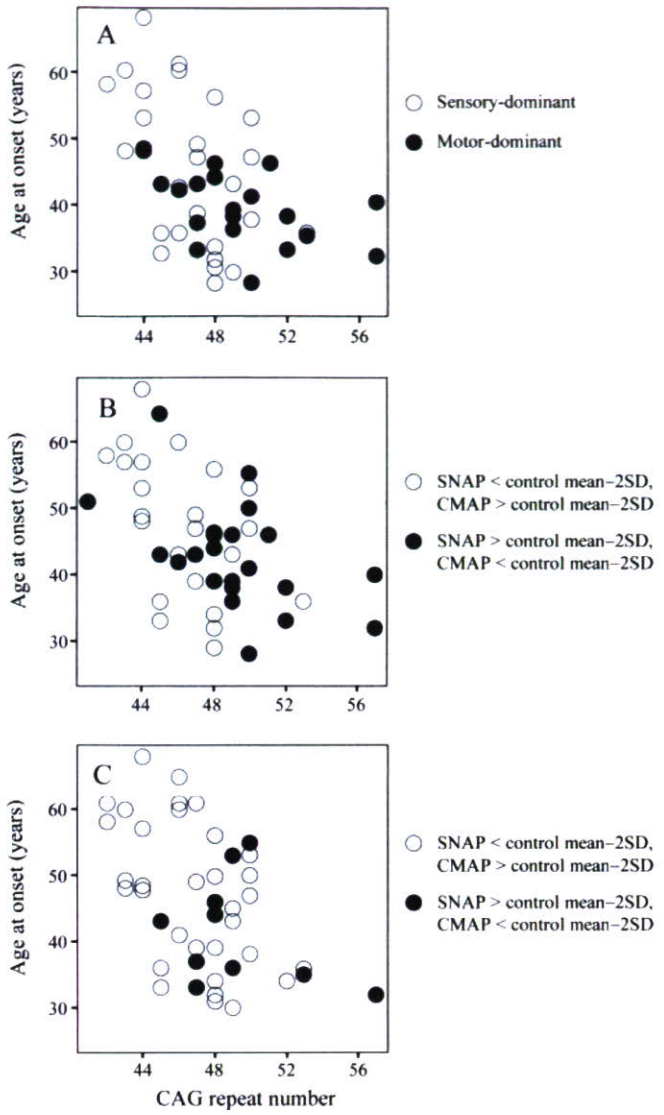

Fig. 3 CAG repeat size determines the age at onset in SBMA. **(A)** Relation between the CAG repeat size and the age at onset according to the phenotypes determined by CMAPs and SNAPs. A longer CAG repeat was closely linked to the motor-dominant phenotype, and a shorter CAG repeat was closely linked to the sensory-dominant phenotype. Motor- and sensory-phenotypes were determined as shown in Fig. IA. **(B)** Relation between the CAG repeat size and the age at onset according to the phenotype determined by using CMAPs and SNAPs in the median nerve. **(C)** Relation between the CAG repeat size and the age at onset according to the phenotype determined by using CMAPs and SNAPs in the ulnar nerve.

sensory discrepancy. Our present findings in SBMA patients strongly suggest that the phenotypic diversity determined by CAG repeat size is a common feature shared by various polyglutamine diseases.

Although the pathological mechanism by which CAG repeat size influences clinical phenotype is unknown, a common molecular basis appears to underlie the heterogeneity of clinical presentations in polyglutamine diseases. The polyglutamine tract encoded by an expanded CAG repeat forms a β-sheet structure, leading to conformational changes and the eventual accumulation of causative proteins (Perutz *et al.*, 2002; Sakahira *et al.*, 2002). Since the propensity of aggregation is dependent on CAG repeat size, the different length of polyglutamine tract may result in a CAG repeat size-dependent pathology.

The observations that a longer CAG repeat results in the motor-dominant phenotype, while a shorter CAG leads to the sensory-dominant presentation, are further reinforced by results of previous studies on the cell-specific histopathological changes in SBMA. A diffuse loss and atrophy of anterior horn cells accompanied by a mild gliosis is characteristic of SBMA (Kennedy *et al.*, 1968; Sobue *et al.*, 1989), suggesting that the pathology of spinal motor neurons is neuronopathy. On the other hand, no substantial neuronal loss in the DRG despite severe axonal loss in the central and peripheral rami suggests that the pathology of sensory neurons is distally accentuated axonopathy, although the primary pathological process may be present in the perikarya of sensory neurons (Sobue *et al.*, 1989; Li *et al.*, 1995). Moreover, the accumulation of mutant AR, a pivotal feature of SBMA pathology, is also different in motor and sensory neurons (Adachi *et al.*, 2005). Mutant AR accumulates diffusely in the nucleus of spinal motor neurons, but cytoplasmic aggregation is predominant in sensory neurons within the DRG (Adachi *et al.*, 2005). The extent of diffuse nuclear accumulation of mutant AR in motor neurons is closely related to CAG repeat size, providing a molecular basis for the present observations that patients with a longer CAG repeat show a greater decrease in CMAPs. On the other hand, the results of anti-polyglutamine immunohistochemistry in this study indicate that cytoplasmic aggregation of mutant AR is more frequent in the patients with a shorter CAG repeat. Taken together, the differential accumulation pattern of mutant AR between motor and sensory neurons, and their differential correlation to CAG repeat size may be the pathophysiological background for the development of motor- and sensory-dominant phenotypes.

In conclusion, the results of the present study are unequivocal electrophysiological phenotypes, motor-dominant, sensory-dominant and non-dominant, especially in young patients of SBMA. These features are dependent on the CAG repeat size within the AR gene, with a longer CAG repeat size is more closely related to the motor-dominant phenotype and a shorter CAG repeat size related to the sensory-dominant phenotype. Our observations shed light on new roles of CAG repeat size in the clinical presentation of SBMA.

Supplementary materials

Supplementary materials are available at *Brain* online.

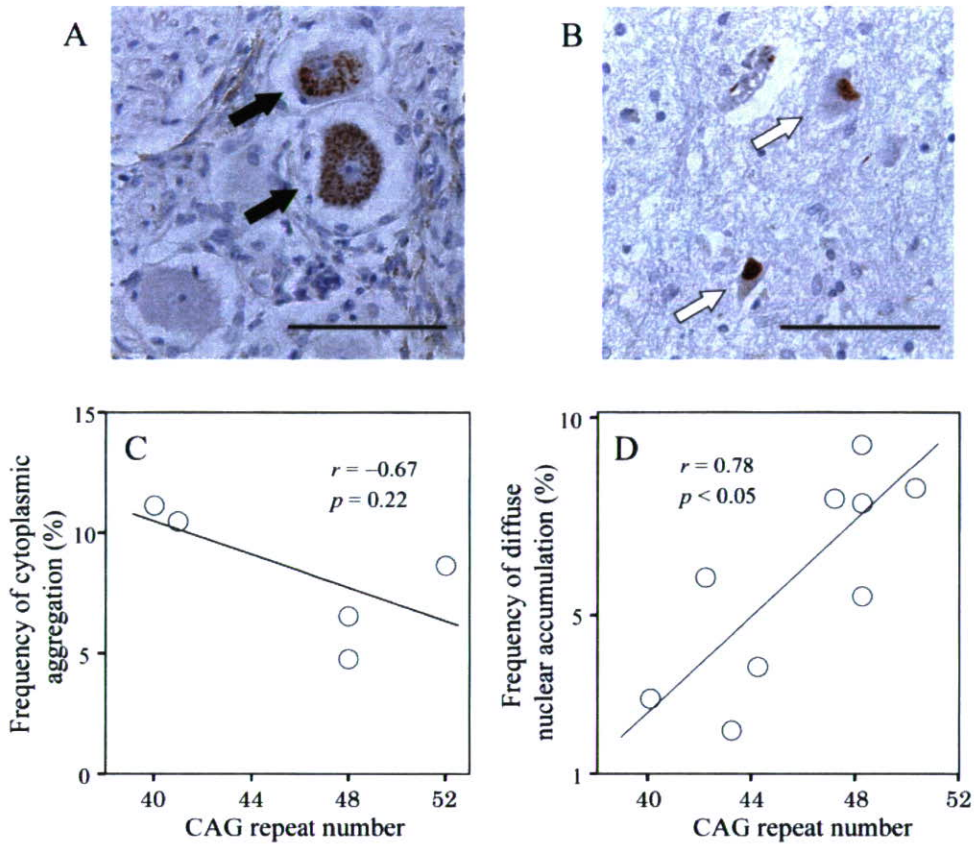

Fig. 4 Immunohistochemical analyses of mutant androgen receptor (AR) accumulation in the dorsal root ganglion (DRG) and that in the spinal anterior horn of SBMA patients. (**A**) Aggregates of mutant AR in the cytoplasm of DRG neurons (black arrows). Scale bar = 100 μm. (**B**) Mutant AR accumulates in the motor neuron nuclei (white arrows). Scale bar = 100 μm. (**C**) Relation between the CAG repeat size and cytoplasmic aggregations in the primary sensory neuron. Cytoplasmic aggregation tended to be more frequent in the patients with a shorter CAG repeat. (**D**) Relation between the CAG repeat size and diffuse nuclear accumulation of mutant AR in the spinal motor neuron. Panel D is reconstructed from the previous report (Adachi *et al.*, 2005).

Acknowledgements

This work was supported by a Center-of-Excellence (COE) grant from the Ministry of Education, Culture, Sports, Science and Technology of Japan, grants from the Ministry of Health, Labor and Welfare of Japan, a grant from Japan Intractable Diseases Research Foundation and the Program for Improvement of Research Environment for Young Researchers from Special Coordination Funds for Promoting Science and Technology (SCF) commissioned by the Ministry of Education, Culture, Sports, Science and Technology of Japan.

References

Adachi H, Katsuno M, Minamiyama M, Waza M, Sang C, Nakagomi Y, et al. Widespread nuclear and cytoplasmic accumulation of mutant androgen receptor in SBMA patients. Brain 2005; 128: 659–70.

Andrew SE, Goldberg YP, Hayden MR. Rethinking genotype and phenotype correlations in polyglutamine expansion disorders. Hum Mol Genet 1997; 6: 2005–10.

Antonini G, Gragnani F, Romaniello A, Pennisi EM, Morino S, Ceschin V, et al. Sensory involvement in spinal bulbar muscular atrophy (Kennedy's disease). Muscle Nerve 2000; 23: 252–8.

Atsuta N, Watanabe H, Ito M, Banno H, Suzuki K, Katsuno M, et al. Natural history of spinal and bulbar muscular atrophy (SBMA): a study of 223 Japanese patients. Brain 2006; 129: 1446–55.

Banno H, Adachi H, Katsuno M, Suzuki K, Atsuta N, Watanabe H, et al. Mutant androgen receptor accumulation in spinal and bulbar muscular atrophy scrotal skin: a pathogenic marker. Ann Neurol 2006; 59: 520–6.

Chevalier-Larsen ES, O'Brien CJ, Wang H, Jenkins SC, Holder L, Lieberman AP, et al. Castration restores function and neurofilament alterations of aged symptomatic males in a transgenic mouse model of spinal and bulbar muscular atrophy. J Neurosci 2004; 24: 4778–86.

Doyu M, Sobue G, Mukai E, Kachi T, Yasuda T, Mitsuma T, et al. Severity of X-linked recessive bulbospinal neuronopathy correlates with size of the tandem CAG repeat in androgen receptor gene. Ann Neurol 1992; 32: 707–10.

Ferrante MA, Wilbourn AJ. The characteristic electrodiagnostic features of Kennedy's disease. Muscle Nerve 1997; 20: 323–9.

Fischbeck KH. Kennedy disease. [Review]. J Inherit Metab Dis 1997; 20: 152–8.

Gatchel JR, Zoghbi HY. Diseases of unstable repeat expansion: mechanisms and common principles. Nat Rev Genet 2005; 6: 743–55.

Guidetti D, Vescovini E, Motti L, Ghidoni E, Gemignani F, Marbini A, et al. X-linked bulbar and spinal muscular atrophy, or Kennedy disease: clinical, neurophysiological, neuropathological, neuropsychological and molecular study of a large family. J Neurol Sci 1996; 135: 140–8.